

Review

Artificial Intelligence and Machine Learning in the Diagnosis and Prognosis of Diseases Through Breath Analysis: A Scoping Review

Christos Kokkotis ¹, Serafeim Moustakidis ¹, Stefan James Swift ², Flora Kontopidou ³, Ioannis Kavouras ⁴, Anastasios Doulamis ⁴ and Stamatis Giannoukos ^{2,*}

¹ AIDEAS OÜ, 10117 Tallinn, Estonia; ckokkoti@affil.duth.gr (C.K.); s.moustakidis@aideas.eu (S.M.)

² Department of Chemistry and Applied Biosciences, ETHZ, 8093 Zürich, Switzerland; sswift@org.chem.ethz.ch

³ Mitera Childrens' Hospital, 15123 Athens, Greece; fkontopid@yahoo.gr

⁴ Institute of Communications and Computer Systems, Iroon Polytechniou 9, 15773 Zografou, Greece; ikavouras@mail.ntua.gr (I.K.); adoulam@cs.ntua.gr (A.D.)

* Correspondence: stamatis.giannoukos@org.chem.ethz.ch

Abstract

Breath analysis is a non-invasive diagnostic method that offers insights into both physiological and pathological conditions. Exhaled breath contains volatile organic compounds, which act as biomarkers for disease detection, allowing for the monitoring of treatments and the tailoring of medicine to individuals. Recent advancements in chemical sensing, mass spectrometry, and spectroscopy have improved the ability to identify these biomarkers; however, traditional statistical approaches often struggle to handle the complexities of breath data. Artificial intelligence (AI) and machine learning (ML) have revolutionized breath analysis by uncovering intricate patterns among volatile breath markers, enhancing diagnostic precision, and facilitating real-time disease identification. Despite significant progress, challenges remain, including issues with data standardization, model interpretability, and the necessity for extensive and varied datasets. This study reviews the applications of ML in analyzing breath volatile organic compounds, highlighting methodological shortcomings and obstacles to clinical validation. A thorough literature review was performed using the PubMed and Scopus databases, which included studies that focused specifically on the role of machine learning in disease diagnosis and incidence prediction via breath analysis. Among the 524 articles reviewed, 97 satisfied the specified inclusion criteria. The selected studies applied ML techniques, fell within the scope of this review, and emphasize the potential of ML models for non-invasive diagnostics. The findings indicate that traditional ML methods dominate, while ensemble methods are on the rise, and deep learning (DL) techniques (especially CNNs and LSTMs) are increasingly used for classifying respiratory diseases. Techniques for feature selection (such as PCA and ML-based methods) were frequently implemented, though challenges related to explainability and data standardization persist. Future studies should focus on enhancing model transparency and developing methods to further integrate AI into the clinical setting to facilitate early disease detection and advance precision medicine.



Academic Editor: Phillip Olla

Received: 29 September 2025

Revised: 4 November 2025

Accepted: 6 November 2025

Published: 10 November 2025

Citation: Kokkotis, C.; Moustakidis, S.; Swift, S.J.; Kontopidou, F.; Kavouras, I.; Doulamis, A.; Giannoukos, S. Artificial Intelligence and Machine Learning in the Diagnosis and Prognosis of Diseases Through Breath Analysis: A Scoping Review. *Information* **2025**, *16*, 968. <https://doi.org/10.3390/info16110968>

Copyright: © 2025 by the authors.

Licensee MDPI, Basel, Switzerland.

This article is an open access article distributed under the terms and conditions of the Creative Commons Attribution (CC BY) license

(<https://creativecommons.org/licenses/by/4.0/>).

Keywords: volatile organic compounds; artificial intelligence; deep learning; biomarkers; non-invasive diagnostics

1. Introduction

Artificial intelligence (AI) and machine learning (ML) have become transformative tools across biomedical research, particularly in non-invasive diagnostic technologies.

Among these, breath analysis is gaining traction as a promising method for disease detection and prognosis, offering a painless, rapid, and cost-effective alternative to traditional clinical diagnostics. By analyzing volatile organic compounds (VOCs) in exhaled breath, researchers can obtain molecular insights into physiological and pathological states. This review systematically examines the application of AI and ML methods to breath analysis for disease diagnosis and monitoring, aiming to summarize the state of the art, identify methodological trends, and highlight gaps for future research.

1.1. Breath Analysis in Medicine

Breath analysis has emerged as a revolutionary and non-invasive diagnostic tool in modern medicine, providing insights into the physiological and pathological processes of the human body. Exhaled breath contains a complex mixture of inorganic gases, thousands of VOCs, as well as microscopic aerosol particles. These components carry molecular information, which reflects dietary changes, performance of human physical activity, uptake of medication, and exposure to environmental pollutants [1–6]. They also serve as biomarkers for assessing health status and diagnosing diseases. Clinical trials involving breath analysis have steadily increased over the past two decades. In the UK, the cumulative number of such trials rose from approximately 10 in the year 2000 to over 700 by 2025, compared to Switzerland, which reported more than 127 studies during the same period [7]. Similar trends have been observed globally, with studies focusing on (a) identifying specific biomarkers for early disease detection, (b) monitoring breath markers associated with treatment response (e.g., pharmacokinetics), (c) measuring toxic chemical exposure, and d) advancing precision medicine.

Recent advances in chemical sensing tools, along with the development of analytical methodologies [8–11], have facilitated the analysis, screening, and decoding of volatile metabolites produced by complex and interacting biochemical processes that continuously evolve within the human body [12–14]. These metabolites are found in body fluids (such as blood, urine, and saliva), tissues, and human breath, and, for both healthy and diseased individuals, they possess a characteristic molecular profile [1,15]. When a change occurs in response to an external stimulus (such as diet) or due to a change in metabolic processes occurring within the human body, the volatile metabolic profile shifts; some VOCs may decrease while some new VOCs may be generated, creating a unique molecular signature for a specific condition. For example, the concentration of acetone in breath has been shown to correlate with fat loss in healthy individuals [16]. Human exhaled breath, as a dynamic mixture of chemical compounds, depends on individual characteristics such as age, gender, genetic makeup, and exogenous factors including exposure to ambient environmental chemicals that enter the body, namely through inhalation, foodstuffs, physical activity, and medication.

Existing mainstream technologies for the analysis of exhaled breath utilize either standalone or combined mass spectrometry (MS)-based approaches [8,17], ion mobility spectrometry (IMS) [18–22], electronic noses [17], gas chromatography, and laser spectroscopy [23,24]. The most widely used analytical technique for ‘off-line’ breath analysis is gas chromatography combined with MS (GC-MS) [13,25]. GC-MS has been extensively applied in the analysis of breath VOCs and semi-VOCs. A GC-MS system may either contain a hard-ionization source (such as electron impact—EI), which produces mass spectra with a plethora of ion fragments, or alternatively, a soft-ionization system (such as chemical ionization—CI), which can operate either in positive or negative ion production and detection mode and produces less fragmentation by providing a more gentle molecular ionization mechanism. These systems are able to produce clearer mass spectral signatures (protonated molecular ion, deprotonated molecular ion, or adducts) compared to the EI ionization method. Existing breath sampling and collection methodologies usually em-

ploy Tedlar gas sampling bags, gas syringes, and glass or stainless-steel canisters. For most of the aforementioned techniques, sample introduction into the GC injection port may be executed directly using a transfer line or via solid phase microextraction (SPME) fibers [26,27]. Two-dimensional GC × GC coupled with MS has been used to analyze polar and non-polar molecules from exhaled breath [28]. GC-MS has also been coupled with thermal desorption (TD) units. In TD-GC-MS [29], breath samples are collected (with the support of a small low-flow pump) and are absorbed within glass or stainless-steel tubes filled with a sorbent material (or a group of sorbent materials) that have the chemical and physical characteristics required for the trapping of the targeted VOCs of interest. Proton transfer reaction MS (PTR-MS) [30–35], selected ion flow tube MS (SIFT-MS) [35–38], and membrane inlet MS (MIMS) [2,39,40] have also been used for the on-line and off-line analysis of VOCs originating from human breath, and the headspace above human biological fluids or skin, for various applications (biomedical metabolomics, volatileomics, homeland security, search and rescue, doping screening, etc.). Both PTR-MS and SIFT-MS utilize soft ionization approaches using reagent ions formed from a plasma source as precursors for soft ionization. PTR-MS primarily uses H_3O^+ as the dominant precursor, although work by Reinecke et al. (2023) also describes the formation of an improved ion source that can switch between H_3O^+ , O_2^+ , NO^+ , and NH_4^+ [41]. The newest models of the SIFT-MS are now capable of rapid switching between eight different reagent ions (H_3O^+ , OH^- , O^- , O_2^- , O_2^+ , NO^+ , NO_2^- , and NO_3^-) [42]. Both PTR-MS and SIFT-MS allow for the rapid analysis of samples with low limits of detection ($\text{LOD} < 1 \text{ ppt}$) [43]. MIMS is based on a three-stage sample introduction process called pervaporation, during which sample molecules are absorbed onto the surface of a membrane (usually silicon-based, e.g., polydimethylsiloxane—PDMS); they diffuse through and then desorb into the vacuum system of the mass analyzer for ionization, product-ion separation, and detection. Recently, high-resolution MS (i.e., Orbitrap-based systems and time-of-flight (TOF) mass analyzers [44]) coupled to ambient ionization sources, such as direct analysis in real time (DART) [45], atmospheric pressure chemical ionization (APCI) [8], and secondary electrospray ionization (SESI) [46–48], have been applied to the real-time analysis of human breath for disease diagnostic purposes. Volatileomics data may be processed for qualitative purposes, typically using commercial databases such as Wiley or NIST libraries (containing more than 600,000 chemical compounds with well-characterized EI mass spectral signatures), as well as custom in-house libraries.

Additionally, electronic noses utilize chemical sensors and pattern recognition algorithms to detect VOCs in real time, enabling their application in disease diagnosis, including the detection of respiratory conditions and metabolic disorders. IMS is another highly sensitive technique that detects trace levels of VOCs by separating ionized molecules based on their mobility within an electric field, and it is a technique that may also be used for rapid breath analysis for disease detection and environmental monitoring. Laser-based spectroscopy techniques, such as cavity ring-down spectroscopy (CRDS) and tunable diode laser absorption spectroscopy (TDLAS), offer high sensitivity and selectivity in detecting gases like nitric oxide (NO), carbon monoxide (CO), and ammonia (NH₃), which act as biomarkers for several disorders. Similarly, Raman spectroscopy may be used to identify the molecular fingerprints of breath metabolites, making it a promising tool for metabolite monitoring and disease diagnostics.

To date, breath analysis studies have depended on traditional statistical methods to identify correlations between specific VOCs and diseases. For example, studies have shown that elevated levels of certain VOCs (such as benzene, toluene, and ethylbenzene) are associated with lung cancer, while increased levels of NO suggest the incidence of asthma. Traditional statistical methods, including regression analysis and principal component

analysis (PCA), are essential in revealing these correlations. Breath samples, however, contain hundreds or even thousands of VOCs, many of which may interact non-linearly, making it often challenging or even unsuitable to use these statistical methods due to the high dimensionality and complexity of breath data.

The integration of AI, particularly ML, has transformed breath analysis by enabling the detection of complex patterns in VOC profiles. Supervised learning models such as support vector machines (SVMs), random forests (RFs), and neural networks (NNs), can accurately classify breath samples and distinguish between diseased patients (e.g., those with lung cancer) and healthy controls. Unsupervised learning techniques (including clustering and dimensionality reduction) assist in identifying patient subgroups and potential biomarkers. Deep learning (DL) approaches, such as convolutional and recurrent neural networks, further enhance disease classification by modeling intricate and non-linear relationships in breath data. These AI-driven techniques advance non-invasive diagnostics, improving disease detection and prognosis. Despite significant progress in applying ML to breath analysis, challenges remain, including the lack of standardization in data collection, limited model interpretability, and the necessity for large, diverse datasets. Many ML models operate as “black boxes,” complicating the identification of key biomarkers, while most studies depend on small, homogeneous populations.

This scoping review addresses these gaps by providing a comprehensive overview of ML applications in breath VOC analysis, highlighting challenges related to data quality, model transparency, and clinical validation, and proposing future research directions to enhance clinical integration. Building on these motivations, this review aims to explore three key areas: first, the main ML and DL techniques currently applied to breath analysis for disease diagnosis and prognosis; second, how analytical and sensing technologies, such as GC–MS, PTR–MS, SIFT–MS, and electronic noses, are integrated with ML and DL models to improve diagnostic performance; and third, the methodological, interpretability, and standardization challenges that limit the clinical translation of ML-based breath analysis. To address these objectives, the paper is structured as follows: Section 2 describes the materials and methods and search strategy; Section 3 presents the main findings categorized by technology type; Section 4 offers a synthesis and discussion of emerging trends, limitations, and future perspectives; and Section 5 concludes with a summary of implications for clinical practice and future research.

1.2. AI in a Nutshell

AI is a multifaceted field dedicated to replicating and enhancing human intelligence through computational means. It involves developing algorithms and models that enable machines to perform tasks requiring human cognitive functions (e.g., learning, reasoning, problem-solving, perception, and language understanding). AI continually evolves by integrating advancements from disciplines such as computer science, statistics, neuroscience, and cognitive psychology [49]. Within AI, ML focuses on creating algorithms that allow computers to learn from data and improve over time without the need for any human intervention in the learning process or any explicit programming for each task [50,51]. DL, a specialized branch of ML, employs neural networks with multiple layers to model complex patterns in large datasets. DL has achieved significant success in areas such as image and speech recognition, natural language processing, and autonomous systems [52–54]. AI methodologies are increasingly utilized across various domains, including healthcare, finance, transportation, and environmental science, to enhance decision-making, automate processes, and extract actionable insights from vast amounts of data.

In this study, we reviewed numerous AI techniques used for breath VOC analysis for disease detection and classification. The methods range from traditional ML al-

gorithms to advanced DL models, each offering distinct advantages. Feature selection (FS) and engineering—encompassing statistical, ML-based, and dimensionality reduction techniques—are crucial for refining data inputs, enhancing model accuracy, and minimizing computational complexity. Table 1 below categorizes and provides brief explanations of the AI techniques used in breath VOC analysis, facilitating understanding for readers unfamiliar with AI and ML concepts mentioned in this manuscript.

Table 1. Overview of AI, ML, and Statistical Models used in Breath VOC Analysis.

Type	Model	Description
Machine Learning Models	Logistic Regression (LR)	A simple yet effective model for binary classification; assumes a linear relationship between features and outcome.
	Support Vector Machine (SVM)	Finds the best decision boundary in high-dimensional spaces using kernels; effective for small to medium-sized datasets.
	K-Nearest Neighbors (KNN)	A non-parametric method that classifies samples based on their closest training examples; simple but computationally expensive with large datasets.
	Decision Tree (DT)	A tree-based model that splits data into branches; highly interpretable but prone to overfitting without pruning.
	Naïve Bayes (NB)	A probability-based classifier assuming feature independence; works well with high-dimensional data despite its simplifying assumptions.
Ensemble & Boosting Methods	Random Forest (RF)	Constructs multiple decision trees and averages predictions; improves accuracy and reduces overfitting.
	eXtreme Gradient Boosting (XGBoost)	A powerful gradient boosting algorithm that sequentially improves weak models; excels in structured data tasks.
	Regularized Random Forest (RRF)	Adds regularization to RF, preventing overfitting and improving generalization.
	Boosted Generalized Linear Models (BGLM)	Enhances standard GLMs with boosting techniques to improve predictive accuracy.
	Bayesian Additive Regression Trees (BART)	A tree-based ensemble method that models complex interactions probabilistically.
Feature Selection & Dimensionality Reduction	Linear Discriminant Analysis (LDA)	A classification technique that projects data onto a lower-dimensional space while maximizing class separation; useful for well-separated classes.
	Partial Least Squares Discriminant Analysis (PLS-DA)	Similar to LDA but better suited for high-dimensional and collinear data, often used in spectral and biochemical analysis.
	Sparse Partial Least Squares (sPLS)	A variant of PLS that introduces sparsity for better feature selection and interpretability.
	Adaptive LASSO	A regularization technique that enhances feature selection by penalizing less important variables.
	Orthogonal PLS-DA (OPLS-DA)	An improved version of PLS-DA that separates predictive information from uncorrelated (orthogonal) variation, improving interpretability.
Deep Learning (DL) & Neural Networks	Weighted Discriminative ELM (WDELM)	Enhances extreme learning machines by assigning importance weight to features for better classification.
	Convolutional Neural Networks (CNN)	Designed for spatial data, commonly used in image analysis and pattern recognition in breath analysis.
	Deep Neural Networks (DNN)	General multi-layered neural networks capable of modeling complex relationships.
	Multilayer Perceptrons (MLP)	A type of fully connected feedforward neural network for structured data classification and regression.
	Recurrent Neural Networks (RNN)	Designed for sequential data, useful for analyzing time-series breath signals.
Probabilistic & Bayesian Models	Long Short-Term Memory (LSTM)	An advanced RNN that captures long-term dependencies in sequential data; well-suited for time-series analysis.
	Gated Recurrent Units (GRU)	A computationally efficient alternative to LSTM with similar performance in sequential tasks.
	Autoencoder Neural Networks	Used for feature learning and dimensionality reduction in an unsupervised manner.
	Hybrid Models (e.g., CNN-XGBoost)	Combines deep learning (CNN) with traditional ML (XGBoost) to leverage the strengths of both techniques.
	Transfer Learning Techniques	Uses pre-trained deep learning models adapted for specific tasks to improve performance with limited data.
Graph Convolutional Networks (GCN)	Graph Convolutional Networks (GCN)	Extends CNNs to analyze relationships in graph-structured data, useful for modeling complex biomedical interactions.
	Bayesian Networks (BN)	A graphical model that represents probabilistic relationships among variables, allowing for uncertainty modeling.
	Bayesian Additive Regression Trees (BART)	A Bayesian tree ensemble method that provides uncertainty estimates alongside predictions.
	Fuzzy-based Quantum Neural Networks (F-QNN)	Integrates fuzzy logic with quantum computing for complex pattern recognition; experimental in biomedical applications.

Table 1. Cont.

Type	Model	Description
Unsupervised Learning	Principal Component Analysis (PCA)	Reduces dimensionality while preserving variance, commonly used for pattern recognition.
	Isolation Forest Algorithm	Identifies outliers by isolating anomalies in feature space, useful for detecting rare disease patterns.
	Hybrid Heat Maps	Combines clustering techniques with visualization for intuitive representation of complex datasets.

2. Materials and Methods

This study did not require ethical approval. Following the Joanna Briggs Institute guidelines, this study was registered on the Open Science Framework (OSF) on 18 February 2025 [55]. The research team conducted the scoping review in accordance with the Preferred Reporting Items for Systematic Reviews and Meta-Analyses extension for Scoping Reviews (PRISMA-ScR) 22-item checklist [56]. This comprehensive set of guidelines ensured thoroughness, consistency, and transparency throughout the review process. By adhering to the PRISMA-ScR framework, the study aimed to maintain high methodological standards, ensure transparent reporting of procedures and findings, and enhance the overall reliability and validity of the qualitative synthesis.

2.1. Literature Searches

The comprehensive literature search was systematically conducted using the Scopus and PubMed online databases. In addition to these electronic searches, a manual search was performed to include records sourced from alternative channels. This dual approach ensured the comprehensive incorporation of relevant studies (enhancing the review's thoroughness and breadth). The specific keywords and search phrases used to query the online databases are detailed below:

(((((“machine learning”) OR (“deep learning”)) OR (“artificial Intelligence”)) AND (((“Breath analysis”) OR (VOCs)) OR (“volatile organic compounds”)) OR (“exhaled breath”))) AND ((diseases) OR (infect*)) AND (((diagnosis) OR (detection)) OR (prognosis)) OR (prediction)) OR (predict*)

The inclusion of “artificial intelligence” and “deep learning” alongside “machine learning” in the search terms was deliberate, as DL represents a specialized subset of ML, while AI encompasses broader computational approaches used in diagnostic modeling. This inclusive strategy ensured that all relevant studies applying intelligent algorithms to breath analysis were captured.

2.2. Eligibility Criteria

2.2.1. Inclusion Criteria

The authors focused exclusively on articles published in peer-reviewed academic journals to ensure the quality and reliability of the included studies. The literature review was conducted from 1 January 2018 to 18 February 2025, capturing the most recent advancements and research developments in the field. The review explicitly targeted studies that analyzed breath VOCs using AI tools for diagnosing or prognosticating diseases. By narrowing down the inclusion criteria in this manner, the review aims to focus on research that integrates AI methodologies with breath VOCs analysis, thereby providing relevant and up-to-date insights into this specialized area of study.

2.2.2. Exclusion Criteria

Given the rapid progress in big data analytics, the substantial increase in available data, and the widespread use of AI tools in recent years, this review excludes articles published

before 2018 to maintain relevance and focus on contemporary developments. Additionally, several specific types of publications and studies were omitted to streamline the review process and ensure the inclusion of pertinent research. These exclusions encompassed conference proceedings (which often present only preliminary findings) as well as papers not written in English (to maintain linguistic consistency and comprehensibility). Studies that did not involve breath analysis, used non-human subjects, applied non-ML techniques, or focused on tasks unrelated to diagnosis or prognosis were also excluded as they fall outside the scope of this review. Furthermore, review articles were excluded to prevent redundancy, and any studies with inaccessible full texts were omitted to ensure that all included research could be thoroughly evaluated and analyzed.

The inclusion and exclusion criteria follow established practices from recent scoping and systematic reviews in biomedical AI research [52,53], which similarly restricted studies by date range, human subjects, and peer-reviewed publication status to ensure relevance, methodological rigor, and comparability across studies.

2.3. Data Extraction

The data extraction process was meticulously conducted by two independent reviewers (designated as C.K. and S.M.), who collaborated to screen the titles, abstracts, and full-text versions of the selected studies, ensuring comprehensive coverage and accuracy. Initially, all identified studies were imported into a spreadsheet to facilitate the systematic removal of duplicate records, thereby streamlining the dataset for further analysis. Following this, the reviewers conducted a detailed screening of titles and abstracts to identify articles that generally met the established inclusion criteria, filtering out those that were irrelevant or did not align with the study's focus. In instances of uncertainty or disagreement regarding the relevance of a particular study, C.K. and S.M. engaged in discussions to reach a consensus, ensuring that only studies with clear and relevant contributions were included. Ultimately, studies were incorporated into the qualitative synthesis if they met a comprehensive set of specific requirements. These requirements encompassed various aspects, such as the application domain, the technological approaches used, the nature and type of data analyzed, the number of subjects involved in the study, the ML models employed, the validation methods applied, and the key findings reported. This rigorous data extraction process ensured that the final selection of studies was relevant and methodologically sound, providing a solid foundation for the qualitative synthesis.

3. Results

Following an initial online search, a total of 524 articles were identified after excluding duplicate entries. A subsequent detailed review of the titles and abstracts narrowed this collection down to 144 potentially relevant studies. After applying the specific inclusion criteria, 97 articles met the requirements and were selected for qualitative synthesis. The entire screening process is illustrated in Figure 1, which adheres to the PRISMA-ScR guidelines for systematic reviews.

All the identified studies employed ML techniques for the diagnosis and prognosis of diseases based on the analysis of VOCs in breath. Studies were excluded if they: (i) used only traditional statistical approaches, (ii) did not involve breath analysis, or (iii) did not conduct original quantitative research. The studies included in this scoping review were categorized into four technological groups based on the techniques applied: (a) sensors, (b) spectrometric techniques, (c) spectroscopic techniques and (d) gas chromatography.

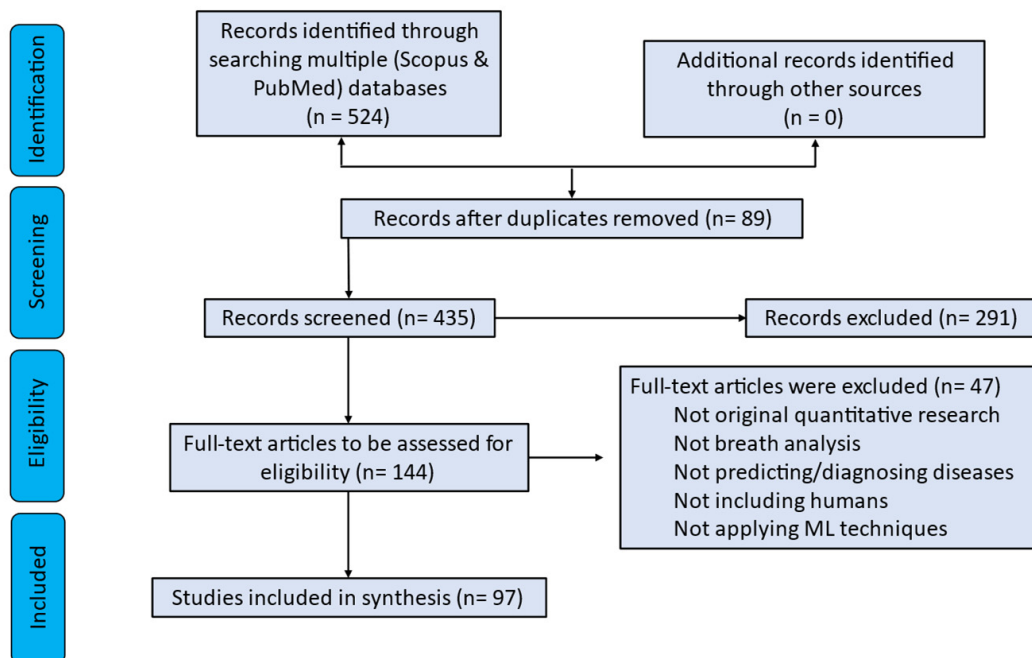


Figure 1. Workflow diagram of screening methodology.

3.1. Sensors

This section provides a comprehensive overview of studies employing eNose sensors and other sensor technologies for breath analysis.

3.1.1. Electronic Noses

This subsection provides a structured overview by organizing studies according to disease type, highlighting the application of eNose sensors in breath analysis for various medical conditions.

Studies related to diabetes focused primarily on distinguishing diabetic patients from healthy controls based on specific breath markers. Gudiño-Ochoa et al. (2024) employed an e-Nose with 7 MOS sensors to detect diabetes using breath analysis [57]. A total of 10,000 data points were obtained from 22 healthy subjects (HS) and 22 patients with diabetes (T1DM or T2DM). FS was performed using a univariate feature selection algorithm and PCA. The XGBoost mode achieved a remarkable accuracy of 95%. Similarly, Bhaskar et al. (2023) used an e-Nose with a TGS 1820 sensor (Figaro Engineering Inc, Mino, Osaka, Japan) to detect acetone levels in 70 diabetic and 82 healthy individuals [58]. With PCA for dimensionality reduction and a deep learning CORNN model combined with SVM, the study reported an accuracy of 98.02%.

In the context of COVID-19, several studies effectively utilized eNoses to identify infected patients based on distinct breath signatures. Li et al. (2023) used an e-Nose system with 64 chemically sensitive nanomaterial sensing elements to analyze the breath of 32 COVID-19-positive (COV+) and 31 COVID-19-negative (COV-) individuals [59]. Using an SVM for classification, the leave-one-out (LOO) validation approach yielded an accuracy of 79%. Doğuç et al. (2023) employed an e-Nose with five air sensors to classify COVID-19 cases from a dataset of 84 negatives and 58 positives [60]. Using gradient-boosted tree algorithms, they achieved 96% accuracy, 95% recall, and 96% precision. Snitz et al. (2021) utilized a PEN3 e-Nose with 10 different thermo-regulated MOS [61]. Using an LSTM model, they obtained a 66.7% Mean TPR in the detection of SARS-CoV-2. Wintjens et al. (2021) [62] also applied an e-Nose with three MOS sensors for COVID-19 detection. Breath samples from 57 COV+ and 162 COV- individuals were

analyzed, with ANN, RF, and LR classifiers achieving a sensitivity of 0.86 and a negative predictive value (NPV) of 0.92, which further improved to 0.96 when combined with clinical variables using LR [62].

For lung cancer (LC), eNose-based studies have mainly aimed to distinguish lung cancer patients from healthy controls through unique VOC signatures. Binson et al. (2021) utilized an e-Nose system with five metal oxide semiconductor sensors for LC detection, reporting an accuracy of 79.31% using XGBoost (R package version 0.4-2) [63]. Furthermore, Binson et al. (2021) used an e-Nose with five chemical gas sensors and a KNN classifier, achieving an accuracy of 91.3% for the same task [64]. In the most recent study, Binson et al. (2024), using LDA, achieved the highest accuracy of 93.14% and an AUC of 0.98, outperforming the previous studies [65]. Another study by Zhao et al. (2021) analyzed 84 LC patients and 40 controls using an e-Nose with 20 gas sensor arrays [66]. The WDELM model achieved an accuracy of 88.71% with leave-one-out cross-validation (LOOCV). In the same task, Lee et al. (2021) employed a D2pNose system and a CNN classifier and reported a classification success rate for LC of over 86% [67]. Kononov et al. (2019) applied an e-Nose with 6 MOS sensors for LC detection [68]. Using LR for classification, the model achieved 97.2% accuracy. Huang et al. (2018) used the Cyranose320 e-Nose system (Sensigent, Baldwin Park, CA, USA), composed of 32 CP sensors, to detect LC [69]. An AUC of 0.90 on external validation was achieved using a non-linear SVM.

For asthma detection, studies primarily aimed to distinguish asthmatic subjects from healthy individuals based on distinctive patterns in breath profiles. Rivai et al. (2024) used an e-Nose system with seven gas sensors to differentiate 30 asthmatic subjects from 30 healthy individuals [70]. Using DL techniques, such as CNN, the study achieved an accuracy of 97.8% [70]. Abdel-Aziz et al. (2020) employed the SpiroNose platform with seven MOS sensors to analyze breath from 655 participants across four cohorts, including children and adults with asthma [71]. The study applied GMB for FS and unsupervised learning of the BNs, achieving an ROC-AUC of 0.72. In another study, Aulia et al. (2023) used an e-Nose with 7 sensors and a 1D-CNN, reporting an accuracy of 96.6% [72].

In chronic obstructive pulmonary disease (COPD)-related research, eNose sensors have been extensively utilized to differentiate COPD patients from healthy controls and patients with other pulmonary conditions. Aulia et al. (2024) employed an e-Nose system with 20 gas sensors for COPD detection, achieving an accuracy of 97.5% using a GCN for classification [73]. In comparison, Binson et al. (2021) used an e-Nose system with five metal oxide semiconductor sensors, achieving an accuracy of 76.67% with the XGBoost classifier [63]. Furthermore, Binson et al. (2021) implemented an e-Nose with five chemical gas sensors and an SVM classifier, achieving a higher accuracy of 90.9% for the same task [64]. Peng et al. (2024) assessed lung health using an e-Nose equipped with eight sensors (WOLF Breath E-nose, Warwick, UK), analyzing 20 COPD patients, four smokers, and 10 healthy individuals [74]. By utilizing Shapley Additive Explanations (SHAP) and PPSDE, they accomplished an accuracy of 96.41%.

Various other diseases have also been studied using eNose systems, showcasing their potential applicability across multiple clinical scenarios. Tozlu et al. (2025) examined psoriasis diagnosis with an e-Nose featuring 22 gas sensors, incorporating demographic, lifestyle, and physical attributes information alongside 60,000 data points per sensor [75]. By employing Gradient Boosting and ExtraTreesClassifier, they achieved an accuracy rate of 96.1%. Jian et al. (2024) investigated urinary bladder cancer (UBC) diagnosis utilizing SEM and ATR-FTIR to analyze Polyaniline (PANI) thin films [76]. Using TC-Sniffer, which integrates CNNs and Transformers, they attained an accuracy of 92.95%. Gómez et al. (2024) explored prostate cancer detection via an e-Nose with 15 gas sensors to analyze

breath and urine, along with an e-Tongue for urine analysis [77]. By applying an SVM classifier, they reached an accuracy of 97.35%.

Ghani et al. (2023) utilized an e-Nose for the early detection of lung disorders, employing an LSTM classifier and achieving an accuracy of 93.59% [78]. Dokter et al. (2023) investigated the use of an e-Nose system (The eNose Company, Zutphen, The Netherlands) with three metal oxide semiconductor (MOS) sensors for diagnosing cervical high-grade squamous intraepithelial lesions (HSIL) [79]. Using an RF classifier and leave-10%-out cross-validation, they reported a sensitivity of 88%, a specificity of 92%, a positive predictive value (PPV) of 92%, and a negative predictive value (NPV) of 89%. Ketchanji Mougang et al. (2023) employed an e-Nose with 11 quartz crystal microbalance sensors for tuberculosis detection, achieving an accuracy of 88%, a sensitivity of 90.8%, a specificity of 85.7%, and an area under the curve (AUC) of 0.88 using an LDA classifier [80]. Xuan et al. (2022) utilized an e-Nose with 16 organic nanofiber sensors to detect silicosis among 221 silicosis miners and 398 non-silicosis miners [81]. By employing multiple classifiers, including RF, XGBoost, KNN, and SVM, the study reported accuracy ranges of 81.7% to 98.7%. Malikhah et al. (2022) used an e-Nose system with five semiconductor gas sensors to detect viral respiratory infections, achieving an accuracy of 94.0% with the fully connected deep convolutional network (FDCN) [82]. Lastly, Binson et al. (2021) worked on detecting pulmonary diseases, achieving accuracies of 91.74% for LC, 89.84% for COPD, and 70.66% for asthma diagnosis using kernel principal component analysis (KPCA) and the XGBoost classifier [83]. Table 2 summarizes the studies utilizing electronic noses for breath analysis in disease diagnostics.

Table 2. Studies using electronic noses.

Author	Year	Application Domain	Breath Analysis Technique	Subjects	Feature Engineering	Best Machine Learning	Validation	Best Results
Tozlu et al. [75]	2025	Diagnosis of Psoriasis	22 gas sensors	143 with psoriasis and 120 HS (BS: 263)	Gradient Boosting	ExtraTreesClassifier	Hold-out (80/20%)	96.1% Acc
Jian et al. [76]	2024	Diagnosis of urinary bladder cancer (UBC)	SEM and ATR-FTIR analyzed PANI thin films in an e-Nose.	76 with UBC and 18 healthy	-	TC-Sniffer, which incorporates CNNs and Transformers	Training (80%)/Testing (20%)	92.95% Acc
Gómez et al. [77]	2024	Detection of prostate cancer	15 gas sensors	66 patients and 47 controls	PCA and discriminant function analysis (DFA)	SVM	5-fold CV	97.35% Acc
Binson et al. [65]	2024	Detection of LC	5 MOS sensors	22 with LC and 40 HS (BS: 248)	Dimensionality reduction with PCA	LDA	5-fold CV	93.14% Acc and AUC of 0.98
Peng et al. [74]	2024	Evaluation of lung health	e-Nose equipped with 8 sensors	20 with COPD, 4 smokers, and 10 HS (BS: 68)	SHAP	PPSDE	5-fold CV	96.41% Acc
Gudiño-Ochoa et al. [57]	2024	Detection of Diabetes	e-Nose equipped with 7 MOS	22 HS and 22 T1DM or T2DM (BS: 44)	Univariate FS algorithm and PCA	XGBoost	Hold-out (55/45%)	95% Acc
Aulia et al. [73]	2024	Detection of COPD	e-Nose with 20 semiconductor gas sensors	30 healthy and 40 with COPD (BS: 70)	PCA	GCN	5-fold CV	97.5% Acc
Rivai et al. [70]	2024	Detection of Asthma	e-Nose with 7 gas sensors	30 healthy and 30 asthmatic suspects (BS: 360)	RF, XGBoost, SVM, PCA, Firefly algorithm	1D-CNN	k-fold CV	97.8% accuracy for CNN
Aulia et al. [72]	2023	Detection of Asthma	e-Nose with 7 sensors	60 subjects: 30 HS, 10 controlled asthma, 10 partly controlled asthma, 10 uncontrolled asthma.	Genetic Algorithm with SVM	1D-CNN	Stratified 5-fold CV	96.6% acc, 96.1% pre, 95.5% recall, and 95.6% F1-score (1D-CNN)
Bhaskar et al. [58]	2023	Detection of Diabetes	e-Nose with TGS 1820 sensor	70 diabetes and 82 HS	-	Deep hybrid CORNN model with SVM	152 samples for validation	98.02% Acc

Table 2. Cont.

Author	Year	Application Domain	Breath Analysis Technique	Subjects	Feature Engineering	Best Machine Learning	Validation	Best Results
Ghani et al. [78]	2023	Early Detection of Lung Disorders	e-Nose (16 sensors)	594 subjects analyzed: 186 HS, 207 COVID-19 infected, 201 with other lung infections.	IG and SUFS algorithms	LSTM	Hold-out (80/10/10%)	93.59% acc, 89.59% sen, 94.87% spe and 0.96 AUC
Doğuç et al. [60]	2023	Diagnosis of COVID-19	e-Nose with 5 air sensors	84 cases in negatives, and 58 cases resulted in positives (BS: 294)	-	Gradient Boosted Trees Learner Algorithm	Hold-out: 90/10% and 75/25%.	96% Acc, 95% recall and 96% precision
Ketchanji Mougang et al. [80]	2023	Diagnosis of Tuberculosis (TB)	11 QMB	46 TB, 38 CON, and 16 TB suspects (BS: 100)	PCA	LDA	Hold-out (70/30%)	88% Acc, 90.8% Sen, 85.7% Spe, AUC of 0.88
Li et al. [59]	2023	Detection of COVID-19	e-Nose: 64 chemically sensitive nanomaterial sensors.	32 COV+ and 31 COV- subjects (BS: 63)	PCA	LG and SVM	LOO	79% Acc
Dokter et al. [79]	2023	Diagnosis of Cervical HSIL	e-Nose contains 3 MOS	25 patients with HSIL and a group of 26 controls	-	RF	L-10%-OCV	88% Sen, 92% Spe, 92% PPV, 89% NPV
Xuan et al. [81]	2022	Diagnosis and early detection of Silicosis	e-Nose with 16 organic nanofiber sensors	398 non-silicosis miners and 221 silicosis miners/Early detection model: 85 patients in stage I as cases, 398 non-silicosis	Linear regression/ PCA/PLS-VIP analysis	RF, XGBoost, KNN and SVM	5-fold CV	81.7–98.7% Acc
Malikhah et al. [82]	2022	Detection of Viral Respiratory Infections	e-Nose consisting of 5 semiconductor gases	353 negative & 306 positive data (BS: 659)	Statistical parameters FDCN	FDCN	Stratified 5-fold CV	94.0% acc, 96.7% sen and 91.5% spe
Lee et al. [67]	2021	Diagnosis of LC	D2pNose	31 HS and 31 LC (BS: 558)	t-SNE, Neural pattern separation, HCA	CNN	Hold-out (80/20%)	>75% diagnostic success, >86% classification success.
Binson et al. [83]	2021	Detection/ Classification of Pulmonary Diseases	e-Nose with 8 sensors	48 LC, 52 COPD, 55 asthma and 63 CON (BS: 218)	KPCA	XGBoost	3-fold CV	LC: Acc: 91.74% COPD: Acc: 89.84% Asthma: Acc: 70.66%,
Zhao et al. [66]	2021	Detection of LC	eNose with 20 gas sensor arrays with conformal gas chambers	84 LC and 40 CON (BS: 124)	TRC algorithm/PCA	WDELM	LOOCV	88.71% Acc
Binson et al. [63]	2021	Detection of COPD and LC	e-Nose system with 5 metal oxide semiconductor-type gas sensors	93 controls, 55 COPD patients, and 51 LC patients (BS: 199)	KPCA	XGBoost	Hold-out (80/20%)	79.31% acc (LC) and 76.67% acc (COPD)
Binson et al. [64]	2021	Detection of COPD and Lung Cancer	e-Nose with five chemical gas sensors	32 LC, 38 COPD patients, and 72 CON (BS: 142)	PCA	KNN, SVM	k-fold CV	LC (KNN): Acc 91.3% COPD (SVM): Acc 90.9%
Snitz et al. [61]	2021	Detection of SARS-CoV-2	PEN3 e-Nose with 10 different thermo-regulated MOS	503 individuals of whom 27 were positive (BS: 503)	PCA	LSTM	LOOCV × 500 times	66.7% Mean TPR
Wintjens et al. [62]	2021	Diagnosis/ Detection of SARS-CoV-2	e-Nose with 3 microhotplate MOS	219 subjects: 57 COVID-19 positive, 162 COVID-19 negative.	-	LR	L-10%-OCV	NPV: 0.96
Abdel-Aziz et al. [71]	2020	Diagnosis of Asthma	eNose platform with 4 differently developed e-Noses and SpiroNose (7 MOS sensors)	601 adults/ school-aged children with asthma, 54 preschool children with wheezing (4 cohorts).	-	GBM/Unsupervised learning of the BNs	Hold-out (75/25%)	ROC of 0.72

Table 2. Cont.

Author	Year	Application Domain	Breath Analysis Technique	Subjects	Feature Engineering	Best Machine Learning	Validation	Best Results
Kononov et al. [68]	2019	Diagnosis of LC	e-Nose multisensory system consisting of 6 MOS	65 with LC and 53 HS (BS: 118)	PCA/Sensor importance observed in the RF and LR classifier	LR	Hold-out (70/30%)	95.0% sen, 100.0% spe, 97.2% Acc
Huang et al. [69]	2018	Detection of LC	E-nose Cyranose320: 32 nanocomposite conducting polymer sensors.	56 LC and 188 non-tumor resections (BS: 244 x 10 times)	PCA	LDA and non-linear SVM	Hold-out (80/20%); external validation (n = 41).	AUCs of 0.91 by LDA and 0.90 by SVM (external validation)

3.1.2. Other Sensors

This subsection categorizes studies by disease type and summarizes how various sensor technologies have been applied for breath-based disease detection.

Multiple studies have utilized sensors to diagnose and predict COPD. Mahdavi et al. (2024) employed STMS techniques, achieving an accuracy of 80.6% using a linear SVM classifier after feature analysis [84]. Karthick et al. (2023) developed an IoT-Spiro system with gas sensors and a hybrid F-QNN model, reporting a high accuracy of 96% [85]. Avian et al. (2022) incorporated an 8-sensor gas device with kernel PCA in combination with several ML classifiers (KNN, DT, LDA, NB, RF, SVM, CB, GB, LGBM, and CNN) and achieved an impressive F1 score of 0.933 [86]. Lastly, El-Magd et al. (2024) utilized transfer learning techniques with pre-trained CNNs such as GoogleNet, achieving a remarkable 100% test accuracy [87]. Furthermore, Suresh et al. (2022) developed a system for predicting COPD, asthma, tuberculosis, and other diseases related to energy expenditure, achieving 100% accuracy with VOC sensors [88]. This comprehensive approach demonstrates the potential of breath-based diagnostics for a wide range of conditions.

Colorectal cancer (CRC), gastric cancer (GC), and LC studies have demonstrated sensor effectiveness by successfully identifying malignancies through distinct breath VOC patterns. Polaka et al. (2023) leveraged a breath analyzer with 73 sensors, analyzing 280 features to differentiate colorectal cancer patients [89]. The study reported an accuracy of 79.3% with an RF classifier, although sensitivity (53.3%) was notably lower than specificity (93.0%). Polaka et al. (2022) used a breath analyzer with gold nanoparticles and MOS sensors to detect gastric cancer, achieving a sensitivity of 66.54% and a specificity of up to 92.39% with an NB classifier [90]. Pérez-Sánchez et al. (2021) used miRNA analysis for lung cancer, achieving a perfect AUC of 1.0 for predicting clinical outcomes [91]. Lee et al. (2024) applied a multimodal gas sensor with a 1D CNN, reporting a sensitivity of 98.9% and an AUC of 0.978 [92]. Lekshmy et al. (2024) explored gas sensors detecting carbon monoxide, acetone, and benzene, achieving an accuracy of 89.39% [93].

Multiple sensor types and ML classifiers have been successfully applied to COVID-19 detection. Nurputra et al. (2022) [94] and Hidayat et al. (2022) [95] both utilized the GeNose C19 system, a device equipped with chemo-resistive MOS sensors, achieving accuracies ranging from 86% to 95% (depending on the classifier used). Shan et al. (2020) employed a nanomaterial-based hybrid sensor array, achieving 95% accuracy in differentiating COVID-19 patients from others with lung infections [96].

Studies addressing additional respiratory and metabolic diseases utilized various sensor technologies with strong performance outcomes. Van der Sar et al. (2023) applied SpiroNose with MOS sensors to diagnose pulmonary sarcoidosis, achieving an accuracy of 87.1% and an AUC of 91.2% [97]. Bhaskar et al. (2024) utilized calibrated MOS gas sensors for ammonia detection in kidney disease patients, achieving 98.37% accuracy using a CNN-CatBoost model [98]. Diabetes detection was explored by Bhaskar et al. (2024) [99] and Lekha et al. (2018), using acetone and MQ-series gas sensors, respectively, achieving accu-

racies ranging from 97.14% to 98% [100]. Baedorf-Kassis et al. (2023) analyzed ventilator waveforms using AI and NNs like ResNet for acute respiratory distress syndrome (ARDS), achieving excellent specificity (>95%) and high F1 scores (>75%) [101]. Wijbenga et al. (2023) employed SpiroNose combined with multivariate LR and dimensionality reduction techniques, attaining a high AUC of 0.94 for chronic lung allograft dysfunction (CLAD) when additional risk factors were incorporated [102]. Table 3 summarizes all the studies that used sensing technologies for breath analysis in disease diagnostics.

Table 3. Summary of studies using various sensing technologies.

Author	Year	Application Domain	Breath Analysis Technique	Subjects	Feature Engineering/	Machine Learning	Validation	Results
Mahdavi et al. [84]	2024	COPD	STMS	34 HS and 33 with COPD (BS: 67)	PCA, F-score, MI regression, recursive feature elimination (RFE), tree-based.	Linear SVM	LOOCV	80.60% Acc, 78.79% Sen, and 82.35% Spe
Lee et al. [92]	2024	LC	Multimodal gas sensor (SENKO, Korea) (10 SMO + 1 PID + 9 EC gas sensor)	74 HS and 107 LC (BS: 181)	-	1D CNN	5-fold CV	98.9% sen, 96.2% spe, and 0.978 AUC of
Lekshmy et al. [93]	2024	LC	3 gas sensors	Pneumonia, TB, and COVID-19 pneumonia	-	SVM		89.39% Acc, 96.6% Sen, 81.29% Spe, 96.4% AUC
Bhaskar et al. [98]	2024	Kidney disease	Calibrated TGS 826 sensor, Tin dioxide (SnO_2), MOS material, integrated heating element.	82 kidney patients and 102 HS (BS: 184)	-	CNN-CatBoost	k-fold CV	98.37% acc
Bhaskar et al. [99]	2024	Type-2 diabetes	TGS 1820 acetone gas sensor	112 non-diabetic and 98 diabetic patients with type 2 diabetes	CNN for feature extraction as proposed methodology, PCA and SVD	CNN-XGBoost	k-fold CV	97.14% Acc
El-Magd et al. [87]	2024	COPD	8 sensors that analyzed exhaled air	COPD 51%, SMOKERS 11%, CON 25% and 13% Air (BS: 78)	Feature extraction based on pre-trained CNN. The CNNs are ResNet 18, ResNet 34, Resnet 50, AlexNet, and GoogleNet.	Transfer learning techniques based on DNNs, 5 pre-trained CNNs + Interpretation by Case-Based Reasoning	Hold-out (90/10%) with internal splitting in Hold-out (80/20%)	GoogleNet: Up to 100% test accuracy, outperformed other pre-trained CNNs.
Baedorf-Kassis M.D. et al. [101]	2023	ARDS	Stand-alone research device that extracts waveforms directly from the ventilator (Memorybox—Hamilton Medical; Bonaduz, Switzerland)	28 patients (BS: 133, 244 breaths were manually analyzed, with 8718 manually identified as reverse-triggers)	-	Resnet	Leave-p-out CV	90.5% Acc
Wijbenga et al. [102]	2023	CLAD	SpiroNose with seven cross-reactive metal-oxide semiconductor sensors.	114 non-CLAD and 38 CLAD (BS: 152)	PLS-DA	LR and multivariate LR	Training set with internal 10-fold CV and validation set were divided by a ratio of 2:1	Improved model (with Risk Factors): AUC 0.94 ($p = 0.04$) BOS vs. RAS: AUC 0.95 Other phenotypes: AUCs ranging from 0.50–0.92 CLAD Stages: AUC 0.56
Karthick and Panka-javalli [85]	2023	COPD	IoT-Spiro System with an array of gas sensors	150 HS and 150 COPD (BS: 300)	Hybrid GBB-BC algorithm, GA, PSO, BBA	F-QNN	10-fold CV	96% acc

Table 3. Cont.

Author	Year	Application Domain	Breath Analysis Technique	Subjects	Feature Engineering/	Machine Learning	Validation	Results
Połaka et al. [89]	2023	Colorectal Cancer	A table-top breath analyzer (73 sensors)	105 with CRC and 186 CON (BS: 291)	Forward selection: evolutionary algorithm or greedy stepwise approach.	RF	Hold-out (50/50%)	79.3% Acc, Sen 53.3%, Spe 93.0% and 0.734 AUC ROC
van der Sar et al. [97]	2023	Sarcoidosis	SpiroNose contains 7 different metal oxide semiconductor sensors (Breathomix, Leiden, The Netherlands)	Pulmonary sarcoidosis: 224; other interstitial lung diseases: 317.	PCA for dimensionality reduction and chi-squared for FS	k-NN, LDA, NN, RF, and SVM	10-fold CV within a 5-fold CV	87.1% Averaged Acc and AUC of 91.2%. RF showed the highest CVA of 87.6%
Nurputra et al. [94]	2022	COVID-19	GeNose C19: 10 metal oxide semiconductor gas sensors.	43 positive and 40 negatives (BS: 615 (330 positive and 285 negative COVID-19))	-	LDA, SVM, stacked MLP, and DNN	Hold-out (70/30%)	88–95% Acc, 86–94% Sen, and 88–95% Spe
Avian et al. [86]	2022	COPD	E-Nose Devices (8 gas sensors)	COPD 20 subjects, 4 SMOKERS and 10 CON (BS: 68)	KPCA with radial basis function as kernel	KNN, DT, LDA, NB, RF, SVM, CB, GB, LGBM and CNN	3-fold CV and 5-fold CV	KPCA contributed to the increasing performance of some classifiers with average F1-Score of 0.933
Hidayat et al. [95]	2022	COVID-19	GeNose C19 with 10 chemoresistive MOS gas sensors	nP = 230 and nN = 230 subjects (BS: 460)	HAC and permutation feature importance	Extra-tree classifier	5-fold CV × 10 times	86% Acc, 88% Sen, 84% Spe
Polaka et al. [90]	2022	GC	Breath analyzer with gold nanoparticle and MOS	54 GC and 85 CON (BS: 139) (JLM Innovation GmbH)	Information Gain, ReliefF, and symmetrical uncertainty	NB	Hold-out (80/20%) × 1000 times	77.8% acc, up to 66.54% sen, up to 92.39% spe.
Suresh et al. [88]	2022	DCOPD, asthma, tuberculosis, cystic fibrosis, obesity-related diseases, energy expenditure disorders.	AGS02MA gas sensor	108	PCA	SVM for diagnosis and Linear Regression for prediction	10-cross-validation strategy, and LOOCV	100% accuracy, 97.5% presentation accuracy (2 misclassifications).
Pérez-Sánchez et al. [91]	2021	LC	miRNeasy Serum/Plasma Kit and GeneChipR miRNA 4.0 Array using A ffymetrix technology (Qiagen, Hilden, Germany)	21 HS and 21 LC (BS: 42)	PCA, Variable importance by RF (Affymetrix, Sunnyvale, Santa Clara, CA, USA)	RF	LOOCV	Lung Adenocarcinoma vs. Squamous Cell Carcinoma: AUC 0.98; Predicting Lung Cancer Outcome (500 Days): AUC 1.0, Spe 100%.
Shan et al. [96]	2020	COVID-19	Nanomaterial-Based Hybrid Sensor Array	49 COVID-19, 58 HS, and 33 non-COVID (printed sensors: SCIONION AG, Berlin, Germany)	-	Linear DFA and quadratic DFA	Hold-out (70/30%)	Patient vs. Control Accuracy: 76% COVID-19 vs. Other Lung Infections Accuracy: 95%
Lekha et al. [100]	2018	Diabetes	MQ-3 and MQ-5 sensors	11 HS, 5 type 1 diabetics and 9 type 2 diabetics (BS: 25) (Huawei Electronics)	Kernel filter weight and then down-sampling through max-pooling, SVD, PCA	1-D CNN	LOOCV	Up to 98% Acc

3.2. Spectrometric Techniques

3.2.1. Mass Spectrometry

Several studies have utilized mass spectrometry techniques to diagnose and differentiate respiratory-related conditions. Fan et al. (2024) employed HPPI-TOFMS to diagnose bronchiectasis using breathomic features from 57 compounds collected from 215 patients with bronchiectasis and 295 controls [103]. Rigorous profile analysis excluded

non-significant and highly correlated compounds, yielding 10 key features. Various classifiers, including RF, LR, XGB, KNN, and DT, were combined into a soft voting ensemble. The study reported an AUC of 0.940, with 90.7% sensitivity, 85% specificity, and 87.4% accuracy on the testing dataset using the RF classifier. Roquencourt et al. (2023) targeted COVID-19 diagnosis using real-time proton transfer reaction time-of-flight mass spectrometry [104]. With PCA and backward RFE for feature selection, RF was used for classification, achieving an AUC of 0.961 (with 98% sensitivity and 74% specificity). Similarly, Liangou et al. (2021) aimed to detect COVID-19 using PTR-ToF-MS and multiple models, including GBMs, reporting 81.2% accuracy. Grassin-Delyle et al. (2021) [105] critically differentiated between COVID-19 patients and non-COVID-19 ARDS cases using elastic net, RF, and SVM models, achieving accuracies ranging from 89% to 93% [106]. Weber et al. (2023) aimed to distinguish allergic asthma using SESI-HRMS, analyzing 375 significant mass-to-charge features [107]. Boruta was applied for FS, and SVMs achieved an accuracy of 78% and an AUC of 0.83. Fu et al. (2023) utilized real-time HPPI-TOFMS for the detection of pulmonary tuberculosis [108]. The breathomics-based model achieved an AUC of 0.975, with 92.6% accuracy, 91.7% sensitivity, and 93.0% specificity. For distinguishing TB from other pulmonary diseases, the model achieved an AUC of 0.961, with an accuracy of around 91.2%. Rai et al. (2022) used FT-ICR-MS specifically for lung cancer diagnosis, achieving 92% accuracy using SVM-RFE. Similarly, Tsou et al. (2021) [109] targeted LC detection with SIFT-MS, reporting an accuracy of 89% (with a sensitivity of 82% and a specificity of 94%) with XGBoost [110]. Butcher et al. (2018) also attempted LC detection with SIFT-MS but achieved lower accuracies of 56% to 74% with MLPs and clamped-ESNs [111]. Chen et al. (2019) utilized high-resolution orbitrap mass spectrometry specifically for tuberculosis detection, identifying optimal segregation features near the positive ion mode at 300 [112].

Several studies have applied MS techniques specifically to detect and monitor chronic metabolic and cognitive diseases. Zhang et al. (2024) utilized HPPI-TOFMS to diagnose and monitor breast cancer progression in a cohort of 937 patients and 1044 controls [113]. Following a four-step VOC product ion filtering process, the optimal features were analyzed using RF, LR, and XGB. The study achieved a sensitivity of 85.9%, a specificity of 90.4%, and an AUC of 0.946. For progression, the AUC values were 0.840 for lymph node metastasis and 0.708 for TNM staging differentiation. Mustafina et al. (2024) specifically targeted cystic fibrosis detection by employing PTR-TOF-MS to analyze breath samples from 102 cystic fibrosis patients and 97 controls [114]. By utilizing LASSO LR and XGBoost, the study achieved AUCs of 0.988 and 0.975 for forced expiratory maneuvers and quiet breathing, respectively. Sensitivities ranged from 88.7% to 93.8%, while specificities ranged from 91.2% to 96.1%. Jiao et al. (2023) aimed to detect cognitive dysfunction using HPPI-TOFMS among 263 patients and 263 controls [115]. A statistical feature selection approach identified relevant features, and classifiers including RF, SVM, LR, XGB, KNN, and DT achieved an AUC of 0.876.

Additional studies have utilized MS techniques to effectively differentiate between liver diseases and psychiatric conditions. Miller-Atkins et al. (2020) applied SIFT-MS to distinguish liver diseases from pulmonary hypertension, achieving 85% classification accuracy using RF [116]. Notably, the sensitivity for detecting hepatocellular carcinoma (HCC) was 73%, outperforming AFP tests. Henning et al. (2023) aimed to differentiate psychiatric disorders (schizophrenia and major depressive disorder) using proton transfer-reaction mass spectrometry [117]. Logistic regression and the BART algorithm achieved accuracies of 76.8% for MDD versus healthy controls, 83.6% for schizophrenia versus healthy controls, and 80.9% for MDD versus schizophrenia. Table 4 summarizes all the studies that employed MS-based methodologies for breath analysis in disease diagnostics.

Table 4. Studies using mass spectrometry.

Author	Year	Application Domain	Breath Analysis Technique	Subjects	Feature Engineering	Machine Learning	Validation	Results
Fan et al. [103]	2024	Bronchiectasis	HPPI-TOFMS	215 with BE and 295 CON (BS: 510)	Non-significant features excluded; correlated compounds removed (>0.9). RF model ran 100 times; top 10 features retained.	RF	Hold-out (50/20/30%)	AUC of 0.940, 90.7% sen, 85% spe, and 87.4% acc
Zhang et al. [113]	2024	Breast Cancer	HPPI-TOFMS	937 women with BC and 1044 CON (BS: 1981)	VOC ions filtered in four steps: exclusion ($p > 0.05$), removal (correlation > 0.9), elimination (AUC < 0.5 via adversarial learning), and RF-based selection.	RF, LR, XGB	Hold-out (50/20/30%)	Sensitivity: 85.9% Specificity: 90.4% AUC: 0.946
Mustafina et al. [114]	2024	Cystic Fibrosis	PTR-TOF-MS	102 CF, 97 CON (BS: 179 quiet breathing, 199 forced expiratory maneuvers).	LASSO LR	XGBoost	5-fold CV	Forced Expiratory Maneuver: AUC: 0.988, Sen: 93.8%, Spec: 96.1% Normal Quiet Breathing: AUC: 0.975, Sen: 88.7% Spec: 91.2%
Roquencourt et al. [104]	2023	COVID-19	Real-time, proton transfer reaction time-of-flight mass spectrometry	67 with COVID-19 and 106 HS (BS: 173)	PCA, Backward RFE	RF	Stratified 5-fold CV \times 4 times	98% sen, 74% spe, 98% NPV, 72% PPV and AUC of 0.961
Weber et al. [107]	2023	Allergic Asthma	SESI-HRMS	48 allergic asthmatics and 56 CON (children)	Boruta FS	SVMs	10-fold CV \times 10 times	78% Acc and AUC of 0.83
Jiao et al. [115]	2023	Cognitive dysfunction	HPPI-TOFMS	1467 subjects: 263 CD, 263 CN controls (PSM-selected from 1204 CN).	A statistical-based FS	RF, SVM, LR, XGB, KNN, and DT	Hold-out (50/20/30%)	AUC of 0.876
Fu et al. [108]	2023	Pulmonary Tuberculosis	Real-time HPPI time-of-flight mass spectrometer	518 PTB and 887 CON (BS: 1405)	FS based on statistical analysis	RF, SVM, LR, XGB, and DT	Hold-out (70 \times 100 times/30%)	Breathomics-Based PTB Detection: 92.6% Acc, 91.7% Sen, 93.0% Spe, AUC: 0.975 VOC Modes for PTB vs. Other Pulmonary Diseases: 91.2% Acc, 91.7% Sen, 88.0% Spe AUC: 0.961
Henning et al. [117]	2023	Schizophrenia and major depressive disorder	proton transfer-reaction mass spectrometry.	36 MDD, 34 schizophrenia and 34 HS (BS: 312)	Using the SPSS software multimodal logistic regression modeling was applied. Additionally, 3 separate logistic regression models were used	BART algorithm	Conditional forward method of SPSS	MDD vs. Healthy Controls: 76.8% accuracy Schizophrenia vs. Healthy Controls: 83.6% accuracy MDD vs. Schizophrenia: 80.9% accuracy
Rai et al. [109]	2022	LC	FT-ICR-MS technology	156 LC, 65 benign pulmonary nodule patients, 193 HS	SVM-RFE, Boot-SVM-RFE	SVM	5-fold CV \times 500 times	92% Acc
Liangou et al. [105]	2021	COVID-19	PTR-ToF-MS	955 samples: 182 positive (88 symptomatic, 27 asymptomatic), 840 negative	Sub-model and compound importance combined to identify the top 20 compounds for COVID-19 prediction	GBM models	Hold-out (70/30%)	81.2% Acc

Table 4. Cont.

Author	Year	Application Domain	Breath Analysis Technique	Subjects	Feature Engineering	Machine Learning	Validation	Results
Tsou et al. [110]	2021	LC	SIFT-MS	148 patients with LC and 168 HS (BS: 316)	Heat map and hierarchical clustering identified several VOC groups	XGBoost	Hold-out (70/30%)	Acc: 89%; Sen: 82%; Spe: 94%; AUC: 0.95
Grassin-Delyle et al. [106]	2021	Critically ill COVID-19 patients	Proton transfer reaction time-of-flight mass spectrometry	28 COVID-19 ARDS and 12 Non-COVID-19 ARDS (BS: 303)	PCA for batch effects, feature selection via elastic net & RF. Features ranked by Wilcoxon p-values, PCA loadings, OPLS-DA importance, elastic net & SVM coefficients, and RF importance.	Linear SVM, elastic net, and RF	Stratified 10-fold CV × 4 times	Elastic net, RF, and SVM achieved an accuracy of between 89% and 93%
Miller-Atkins et al. [116]	2020	Cirrhosis, Primary, and Secondary Liver Tumors	SIFT-MS	296 subjects: 54 no liver disease, 30 cirrhosis, 112 HCC, 49 pulmonary hypertension, 51 colorectal cancer liver metastases.	PCA for batch effects/outliers, logistic regression for metabolite-cohort associations, Gini scores for RF variable importance	RF	LOOCV/(5%) of the patients in each group was testing set	Classification Acc: 85% Balanced Acc: 75% Sen for Detecting HCC: 73% Comparison: AFP Sen was 53% in the same cohort
Chen et al. [112]	2019	Tuberculosis	high-resolution orbitrap mass spectrometry analysis	19 TB patients and 17 non-TB subjects	PCA for visualization, SAM-based FS	SVM	N/A	The best segregation % rate observed when applying feature extraction from positive ion mode near 300
Butcher et al. [111]	2018	LC	SIFT-MS	20 LC and 20 HS (BS: 40)	-	MLPs and clamped-ESNs	5-fold CV	56% to 74% Acc

3.2.2. Hyphenated Mass Spectrometry

Hyphenated mass spectrometry has been employed across numerous diseases, utilizing advanced ML models to enhance diagnostic precision and prognostic capabilities. Below is a synthesis of 19 studies categorized by disease and detailing their methodologies. Taylor et al. (2024) utilized a novel microreactor to analyze 34 carbonyl compounds for pulmonary fibrosis detection [118]. ML models, including SVM, RF, and BGLM, were applied. A five-fold cross-validation process showed that these models achieved an AUROC score of 0.877 for diagnosis and 0.873 for disease severity classification. In the diagnosis of gastrointestinal cancer, Xiang et al. (2023) exploited GC-MS and UVP-TOFMS to distinguish early-stage upper gastrointestinal (UGI) cancer from benign conditions [119]. They analyzed 163 features derived from breath samples and employed RFE for FS. Their models demonstrated exceptional performance using RF, SVM, XGBoost, and LDA, with AUROC scores of 0.959 and 0.994 for exhaled breath analysis, showing comparable results for gastric-endoluminal gas samples.

Several studies have explored COVID-19 diagnosis. Hirdman et al. (2023) employed liquid chromatography-mass spectrometry to analyze 110 proteins per sample and applied RF models for classification, achieving 92% accuracy [120]. Xue et al. (2022) used a portable GC-MS system and implemented SVM, KNN, LR, and ANN with five-fold cross-validation [121]. Their SVM model exhibited superior capability, achieving 97.3% accuracy, 100% sensitivity, and 94.1% specificity. Woollam et al. (2022) adopted HS-SPME GC-MS and utilized LDA models, achieving an impressive ROC AUC of 0.99, with 100% sensitivity and 92% specificity [122]. Zhang et al. (2022) employed HPPI-TOFMS and an XGBoost classifier, reporting 92.2% sensitivity and 86.1% specificity in a three-fold validation approach [123]. For HCC, Nazir et al. (2023) integrated GC-MS with electrochemical analysis, utilizing PCA

and hybrid heat maps to reduce dimensionality [124]. Their unsupervised ML approach yielded a sensitivity of 99% in early HCC detection. In lung cancer, various studies have demonstrated the effectiveness of breath analysis combined with ML. Gashimova et al. (2022) utilized TD-GC-MS to analyze 205 VOCs, employing LR, SVM, RF, and ANN models [125]. Sensitivities ranged from 81% to 88%, with corresponding specificities between 83% and 85%. Koureas et al. (2021) used SPME-GC-MS to evaluate 29 VOCs and employed RF and NB models. Cross-validation yielded an accuracy of 91% and an AUC of 0.96 [126]. Similarly, Koureas et al. (2020) achieved 88.5% accuracy and an AUC of 0.94 using RF models for VOC-based lung cancer detection [127]. In another study, Pelit et al. (2024) applied LightGBM, achieving an accuracy of 81.8% [128].

Cheng et al. (2022) analyzed VOCs from patients using TD-GC-MS to diagnose colorectal adenomas and cancer [129]. Employing isolation forest algorithms and RF models, they validated their approach through LOOCV and testing-validation splits. Depending on the model, sensitivity ranged between 67.3 and 80%, and specificity was 70%, respectively. Patnaik et al. (2022, 2023) employed GC-MS to analyze multiple breath parameters for liver function assessment [130,131]. They utilized SVR, RF, and ensemble tree regression (ETR) models, reporting R-squared values between 0.78 and 0.85 for predictive scores. Models showed accuracy improvements across different validation setups, with precision, recall, and probability scores ranging from 0.84 to 0.94. Khan et al. (2022) utilized 2D GC × GC-TOF-MS combined with OPLS-DA and RF models for insulin resistance detection [132]. Their approach, validated using 10-fold cross-validation and hold-out splits, achieved an AUROC of 0.87 in identifying pre-diabetic conditions among Hispanic adolescents. Di Gilio et al. (2020) employed TD-GC/MS and RF models to detect malignant pleural mesothelioma, achieving a sensitivity of 93% through LOOCV validation [133]. Similarly, tuberculosis detection was pursued by Beccaria et al. (2019) [134] and Bobak et al. (2021) [135]. Beccaria's study employed RF models to analyze 128 features, achieving 100% sensitivity and 60% specificity. Bobak, using Boruta FS with RF, reported an accuracy of 90%. Lastly, Sharma et al. (2021) utilized GC-MS to analyze 103 peaks potentially containing VOCs for asthma detection [136]. Their PCA- and LDA-based models achieved an accuracy of 94.4% in distinguishing between asthma patients and controls. Table 5 summarizes all the studies that used hyphenated MS-based approaches for breath analysis in disease diagnostics.

Table 5. Employed studies by using hyphenated mass spectrometry.

Author	Year	Application Domain	Breath Analysis Technique	Subjects	Feature Engineering	Machine Learning	Validation	Results
Pelit et al. [128]	2024	LC	SPME fiber and GC-MS	70 LC and 96 control (BS:166) in the second phase	Feature Importance of LightGBM	LightGBM	5-fold CV	81.80% Acc
Taylor et al. [118]	2024	Pulmonary fibrosis	A novel microreactor	30 ILD patients: 25 with FEV1 & FVC, 22 with DLCO	PLS-DA analysis, EFS	BGLM, RLR, RRF, SPLS, SVMPoly and RF	5-fold CV	AUROC: 0.877 (diagnosis), 0.873 (disease severity).
Xiang et al. [119]	2023	Early upper gastrointestinal cancer from benign	GC-MS and UVP-TOF-MS	193 subjects: 116 UGI cancer, 77 benign disease/Gastric-endoluminal gas samples: 114 UGI cancer, 76 benign disease	RFE	RF, XGB, SVM, and LDA	Hold-out (70/30%)	Exhaled Breath Models (UGI Cancer vs. Benign): GC-MS: AUC 0.959; UVP-TOFMS: AUC 0.994 Gastric-Endoluminal Gas Models (UGI Cancer vs. Benign): GC-MS: AUC 0.935 UVP-TOFMS: AUC 0.929
Hirdman et al. [120]	2023	COVID-19	Liquid chromatography-mass spectrometry.	20 Patients COV-POS, 16 COV-NEG, and 12 HCO (BS: 40)	Independent FS in Perseus using ANOVA scores	RF	Hold-out (60 × 100 times/40%)	92% Acc

Table 5. Cont.

Author	Year	Application Domain	Breath Analysis Technique	Subjects	Feature Engineering	Machine Learning	Validation	Results
Nazir et al. [124]	2023	Early detection of HCC	GC-MS and Electrochemical analysis	35 with Hepatocellular carcinoma and 30 HS (BS: 325)	PCA and hybrid heat maps	Unsupervised ML, PCA and hybrid heat maps	N/A	99% Sen
Patnaik et al. [130]	2023	Abnormal Liver Function	GC-MS	30 liver patients and 33 HS (BS: 198)	RFE based on DT	NB and RF	Hold-out (70/30%)	Acc: 0.7 to 0.95, Pre: 0.84 to 0.94, Recall: 0.84 to 0.94 Prediction Prob: 0.84 to 0.94
Gashimova et al. [125]	2022	LC	TD-GC-MS	110 LC and 212 HS (BS: 322)	DA	SVM and ANN	K-Fold CV	ANN's Performance: LC vs. Young Healthy: Sen: 88%, Spe: 83% LC vs. Old Healthy: Sen: 81%, Spe: 85%
Xue et al. [121]	2022	COVID-19	A portable gas chromatograph-mass spectrometer.	65 COVID-19 and 57 CON (BS: 122)	PCA	SVM	5-fold CV	Acc: 97.3%, Sen: 100% Spe: 94.1%, Pre: 95.2% F1 Score: 97.6%
Zhang et al. [123]	2022	COVID-19	HPPI-TOF-MS	95 COVID-19 and 106 HS (BS: 201)	-	XGB	Hold-out (50/20/30%)	Sen: 92.2%, Spe: 86.1%
Cheng et al. [129]	2022	Colorectal Adenomas and Cancer	Thermal desorption-gas chromatography coupled with TD-GC-MS	382 FIT-positive patients (Dutch bowel screening): 84 negative controls, 130 non-AAs, 138 AAs, 30 CRCs	Variable importance from RF (model 2) PCoA visualization	Isolation Forest Algorithm, RF	Hybrid: LOOCV and hold-out	CRC vs. Negative Controls: 67.3% Sen, 70% Spe AA vs. Negative Controls (10 VOCs): 79% Sen, 70% Spe CRC vs. Control (Model 2): 80% Sen, 70% Spe AA vs. Control (Model 2): 77% Sen, 70% Spe
Woollam et al. [122]	2022	COVID-19	HS-SPME GC-MS QTOF	12 negative and 14 positive	PCA	LDA	5-fold CV × 1000 times	ROC AUC of 0.99, Sen: 100% and Spe: 92%
Patnaik et al. [131]	2022	Liver function	GC-MS	17 liver patients and 28 HS (BS: 135)	no	Linear regression, SVR, RFR, and ETR.	Hold-out (70/30%)	The R-square value between actual clinical score and predicted clinical score is found to be 0.78, 0.82, and 0.85 for CTP score, APRI score, and MELD score, respectively.
Khan et al. [132]	2022	Insulin resistance in pre-diabetic Hispanic adolescents with obesity.	Two-dimensional GC × GC-TOF-MS	6 normal, 15 insulin resistance and 7 borderline (BS: 112)	OPLS analysis, RF importance	RF regression	10-fold CV/Hold-out (75/25%)	AUC-ROC curve of 0.87, after CV
Koureas et al. [126]	2021	Lung Cancer from Benign Pulmonary Diseases	SPME-GC-MS	49 Ca+ patients, 36 Ca- patients and 52 HS (BS: 137)	Wrapper functions	NB, LR and RF	10-fold CV	Untargeted Analysis (Ca+ vs. HC): Acc 91.0%, AUC 0.96. Targeted Analysis (Ca+ vs. HC): Acc 89.1%, AUC 0.97 Efficiency Improvement (Ca+ vs. Ca-): Acc 52.9% → 75.3%, AUC 0.55 → 0.82
Bobak et al. [135]	2021	Tuberculosis	GC × GC-TOF-MS	10 children with TB disease, 11 had unconfirmed TB, and 10 were unlikely to have TB disease (BS: 31)	Boruta FS	RF	5-fold CV	90% Acc
Sharma et al. [136]	2021	Asthma	GC-mass spectrometry	30 asthma, 8 atopic non-asthma, and 35 non-asthma/non-atopic subjects (BS: 79)	PCA	LDA	Hold-out (63/37%)	94.4% Acc
Koureas et al. [127]	2020	LC	SPME of the VOCs and subsequent gas GC-MS analysis	51 LC, 38 patients with pathological CT findings not diagnosed with LC, and 53 HS (BS: 104)	Weka and the Mann-Whitney tests	RF	10-fold CV	88.5% acc (AUC 0.94).

Table 5. Cont.

Author	Year	Application Domain	Breath Analysis Technique	Subjects	Feature Engineering	Machine Learning	Validation	Results
Di Gilio et al. [133]	2020	Malignant Pleural Mesothelioma	TD-GC/MS	14 MPM and 20 HS	Gini Index	RF	LOOCV	93% Acc
Beccaria et al. [134]	2018	Pulmonary Tuberculosis	Thermal desorption-GC × GC-TOF-MS with chemometric analysis.	50 individuals, including 32 with active pulmonary TB and 18 controls with TB symptoms, but confirmed Mtb negative	'elbow method' where feature importance	RF	5-fold CV × 10 times	100% Sen and 60% Spe

3.2.3. Ion Mobility Spectrometry

Ion mobility spectrometry has proven to be a powerful technique in breath analysis for the detection and diagnosis of various diseases, leveraging its ability to separate and identify VOCs based on their mobility in an electric field. Several studies have combined IMS with advanced ML algorithms to enhance diagnostic accuracy. In the study by Wieczorek et al. (2022), temperature-dependent gas chromatography coupled with field asymmetric ion mobility spectrometry (TD-GC-FAIMS) was utilized to detect liver cirrhosis [137]. The researchers analyzed breath samples from 46 individuals, comprising 35 patients with cirrhosis and 11 healthy controls, resulting in 157 spectra with 3400 discrete ion intensity values each. A 1-D CNN was developed for classification, with stratified 4-fold cross-validation applied for model evaluation and hyperparameter tuning. The dataset was divided into a training set and a validation set, each comprising 82 samples from 24 individuals, and a test set comprising 75 samples from 22 individuals. The model achieved an AUC of 0.90, indicating high discriminatory power between cirrhotic patients and healthy subjects. Furthermore, SHAP was applied to interpret the model's output, offering insights into the importance of individual features and enhancing the model's transparency and interpretability. Thomas et al. (2021) also focused on liver disease detection using TD-GC-FAIMS, analyzing 200 breath samples with 3400 ion intensity values from 50 participants: 35 with cirrhosis, 4 with non-cirrhotic portal hypertension, and 11 healthy individuals [138]. A pre-trained convolutional neural network (ResNet-50) served as the foundation for various ensemble learning models, including RUSBoost, SKNN, GNB, and medium-sized GSVM. A five-fold CV was employed for validation. The molecular feature scores derived from these models increased with cirrhosis severity, achieving an AUC of 0.78. The classifiers demonstrated sensitivity between 88 and 92% and specificity of 75% in detecting the presence or stage of cirrhosis, highlighting the potential of breathomics in liver disease assessment.

Chen et al. (2021) investigated COVID-19 detection using gas chromatography coupled to ion mobility spectrometry (GC-IMS) [139]. The study analyzed VOC profiles, identifying 70 species from breath samples of 191 participants: 74 COVID-19 patients, 30 non-COVID-19 patients with respiratory infections, 56 healthcare workers, and 31 non-COVID-19 controls. ML models, including SVMs, GBMs, and RFs, were utilized for classification. PCA helped assess the weighted importance of VOC species in the models. With a 70/30 training-testing split and an internal stratified 10-fold CV, the models achieved precision rates between 91% and 100% in discriminating COVID-19 patients from others. GBM and RF models effectively distinguished RI patients from healthy subjects with 100% precision, demonstrating the efficacy of VOC-based breath analysis in infectious disease detection. Mentel et al. (2021) focused on oral squamous cell carcinoma detection using GC-IMS, analyzing VOC profiles from breath samples. The study included 105 participants: 55 patients with suspected OSCC before surgery and 50 healthy controls. Various classification algorithms were

applied, including LR, LDA, KNN, DT, GNB, SVM, and RF. A ten-fold CV was used for model evaluation [140]. The models achieved average accuracy rates of between 86% and 90%, suggesting that breath analysis via IMS could be a non-invasive diagnostic tool for early detection of OSCC. Sukaram et al. (2023) explored the diagnosis of hepatocellular carcinoma using GC-FAIMS. The study analyzed [141] breath samples from 343 participants: 124 HCC patients, 124 cirrhosis patients, and 95 healthy volunteers. An algorithm assigned feature importance scores (F scores) to VOCs based on their ability to differentiate among the cohorts. XGBoost was employed for classification, with the dataset split into 80% for training and 20% for testing. Using 9 key VOCs, the model achieved a sensitivity of 70.0%, a specificity of 88.6%, and an overall accuracy of 75.0% in diagnosing HCC. Notably, the acetone dimer emerged as a significant biomarker, achieving an AUC of 0.775, compared to alpha-fetoprotein (AFP), which demonstrated an AUC of 0.714 ($p = 0.001$) in distinguishing early HCC from cirrhotic patients. Additionally, the acetone dimer was effective in classifying treatment responders, with a sensitivity of 95.7%, a specificity of 73.3%, and an accuracy of 86.8%. Table 6 presents all the studies that used IMS for breath analysis in disease diagnostics.

Table 6. Studies employing ion mobility spectrometry.

Author	Year	Application Domain	Breath Analysis Technique	Subjects	Feature Engineering	Machine Learning	Validation	Results
Sukaram et al. [141]	2023	Diagnosis of Hepatocellular Carcinoma	GC-FAIMS	124 HCC, 124 cirrhosis, and 95 HS	F score	XGBoost	Hold-out (80/20%)	HCC Diagnosis (9 VOCs): Sen 70.0%, Spe 88.6%, Acc 75.0% Early HCC vs. Cirrhosis: Acetone Dimer AUC 0.775, AFP AUC 0.714 Acetone Dimer (Treatment Responders): Sen 95.7%, Spe 73.3%, Acc 86.8%
Wieczorek et al. [137]	2022	Detection of Liver Cirrhosis	TD-GC-FAIMS	35 with cirrhosis and 11 HS (BS: 157)	-	1-D CNN, SHAP	Hybrid: Combination of hold-out and 4-fold CV	AUC of 0.90
Thomas et al. [138]	2021	Detection of liver disease	TD-GC-FAIMS	35 with cirrhosis, 4 with non-cirrhotic portal hypertension, and 11 HS (BS: 200)	-	Pre-trained CNN ResNet-50, SC-2A (RUSBT ensemble), SC-1A (SKNN), SC-2B (GNB), RT-4B (Medium GSVM).	5-fold CV	Molecular feature score increased with cirrhosis stage (AUC 0.78). Algorithmic models: Sen 88–92%, Spe 75% for cirrhosis detection/staging.
Chen et al. [139]	2021	Detection of COVID-19	GC-IMS	191 subjects: 74 COVID-19, 30 non-COVID-19, 56 healthcare workers (breath sampling & tracing), 31 non-COVID-19 controls.	PCA, Weighted importance of VOC species in the GBM and RF models	SVMs, GBMs, and RFs	Hold-out (70/30%)	Discrimination Capability: COVID-19 vs. HCW + NC and RI Precision Range: 91% to 100% GBM and RF Models: Discriminated RI Patients from Healthy Subjects Precision: 100%
Mentel et al. [140]	2021	Detection of Oral squamous cell carcinoma	GC-IMS	55 with suspected OSCC before surgery and 50 HS (BS: 92)	-	LR, LDA, KNN, DT, GNB, SVM, RF	10-fold CV	86–90% average Acc

3.3. Spectroscopic Techniques

3.3.1. Laser Spectroscopy

Recent studies demonstrate that laser spectroscopy has become a powerful tool for breath analysis in disease detection and diagnosis. Golyak et al. (2024) employed infrared laser spectroscopy, utilizing a quantum cascade laser and a Herriott multipass gas cell, to analyze breath samples from patients with T1DM, asthma, pneumonia, and healthy

controls [142]. The study included 204 breath samples from 71 healthy participants, as well as 77 patients with T1DM, 32 of whom had asthma and 24 had pneumonia. Feature reduction techniques like PCA, LDA, and variational autoencoders were applied, followed by classification using RF, Multinomial LG, and SVM algorithms. The models achieved up to 100% balanced accuracy, underscoring the robustness of the method in distinguishing between different respiratory conditions. Similarly, Liang et al. (2023) utilized cavity-enhanced direct frequency comb spectroscopy (CE-DFCS) to detect the SARS-CoV-2 infection by analyzing 14,836 molecular absorption features and 16 known small-molecule compounds in breath samples [143]. This study involved 170 participants, including 83 SARS-CoV-2-positive and 87 negative individuals. PLS regression was applied for FS and DA for classification. The model, tested on 30 samples with 10,000 repeated trials, achieved an AUC of 0.849, demonstrating the technique's efficacy in identifying COVID-19 infections through breath analysis.

In another study, Shlomo et al. (2022) applied FTIR spectroscopy combined with BOH system AI algorithms to detect SARS-CoV-2 [144]. Each breath sample provided a vector containing 7882 data points. Validation on 100 proof-of-concept samples revealed that the FTIR/AI algorithm achieved 100% sensitivity and specificity compared to PCR results, indicating a highly accurate non-invasive diagnostic method for COVID-19. Cusack et al. (2024) focused on detecting COVID-19 pneumonia using laser spectroscopy [145]. From normalized breath prints, 191 features were extracted for classification. FS was performed using a variant of the minimum redundancy maximum relevance algorithm, and classification was conducted using a linear SVM. The model achieved a non-nested accuracy of 81.7% (77.4% sensitivity, 85.5% specificity) and a nested accuracy of 72.2% (67.9% sensitivity, 75.8% specificity) using LOOCV.

Borisov et al. (2021) utilized laser optical-acoustic spectroscopy to diagnose acute myocardial infarction by analyzing eight VOCs in the 2.6–10.6 μm range [146]. The study included 72 samples from 30 patients with primary myocardial infarction and 42 healthy participants. PCA was employed for feature reduction, while a linear SVM was used for classification. The model achieved 82% sensitivity and 93% specificity, indicating its potential for the early detection of cardiac events through breath analysis. Additionally, Kistenev et al. (2019) applied laser photoacoustic spectroscopy to diagnose bronchopulmonary diseases, including lung cancer, COPD, and pneumonia [147]. PCA facilitated feature extraction, and an SVM with a radial basis function (RBF) kernel was utilized for classification. The model demonstrated high accuracy in biomarker detection ($\geq 95\%$) and disease classification, achieving specific accuracies of approximately 95.65% for lung cancer, 81.12% for COPD, 84.12% for pneumonia, and 89.46% for healthy individuals. Collectively, these studies underscore the effectiveness of laser spectroscopy combined with advanced ML techniques in accurately diagnosing a range of diseases through breath analysis. Table 7 lists all the studies that employed laser spectroscopy for breath analysis in disease diagnostics.

Table 7. Studies utilizing laser spectroscopy.

Author	Year	Application Domain	Breath Analysis Technique	Subjects	Feature Engineering	Machine Learning	Validation	Results
Golyak et al. [142]	2024	Diagnosis of patients with T1DM, asthma, and pneumonia	Infrared laser spectroscopy	71 HS, 77 with T1DM, 32 with asthma, and 24 with community-acquired pneumonia (BS: 204)	PCA, LDA, Variational autoencoder for dimensionality reduction	RF, Multinomial LG and SVM	Hold-out (80/20%)	Up to 100% Balanced Acc
Cusack et al. [145]	2024	Detection of COVID-19 pneumonia	LAS	53 SARS-CoV-2 Positive and 62 SARS-CoV-2 Negative (BS: 115)	mRMR	Linear SVM	Non-nested and nested LOOCV	A non-nested and nested Acc of 81.7% (77.4% Sen, 85.5% Spe) and 72.2% (67.9% Sen, 75.8% Spe)

Table 7. Cont.

Author	Year	Application Domain	Breath Analysis Technique	Subjects	Feature Engineering	Machine Learning	Validation	Results
Liang et al. [143]	2023	Detection of SARS-CoV-2 infection	CE-DFCS	83 positive and 87 negative (BS: 170)	PLS	DA	Training set (n = 140)/Testing set (n = 30) × 10,000 times	AUC of 0.849
Shlomo et al. [144]	2022	Detection of SARS-CoV-2	FTIR spectroscopy	96 PCR-positive and 201 PCR-negative (BS: 297)	-	BOH system AI algorithm's	100 proof-of-concept samples for validation	100% Sen and Spec
Borisov et al. [146]	2021	Diagnosis of acute myocardial infarction	Laser optical-acoustic spectroscopy	30 with primary myocardial infarction and 42 HP (BS: 72)	PCA	Linear SVM	Hold-out (60/40%) × not less than 500 times	82% sen and 93% spec
Kistenev et al. [147]	2019	Diagnosis of Bronchopulmonary diseases	Laser photoacoustic spectroscopy	9 LC; 12 COPD; 11 pneumonia and 29 CON (BS: 61 × 5 times)	PCA	SVM with RBF kernel	Random splitting of initial data on teaching and testing sets was × 250 times	Biomarker detection: Acc & selectivity ≥95% Disease detection Acc: LC ~95.65%, COPD ~81.12%, Pneumonia ~84.12%, Healthy ~89.46%

3.3.2. Raman Spectroscopy

Raman spectroscopy has emerged as a valuable tool for disease diagnosis through breath analysis, as demonstrated by two recent studies. Xie et al. (2024) targeted the diagnosis of lung and gastric cancer using SERS spectra obtained from exhaled breath [148]. They employed a plasmonic metal–organic framework nanoparticle (PMN) film to collect the breath samples in a study involving 1780 samples from 79 subjects, which included 49 healthy individuals, 22 lung cancer patients, and 8 gastric cancer patients. Each sample provided 1000 one-dimensional data points. For data processing, PCA was used for feature engineering, while RF classifiers and permutation importance methods were utilized for FS. Classification was conducted using PLS-DA models and a shallow ANN, which achieved an accuracy of 89% in distinguishing healthy individuals from lung and gastric cancer patients. The second study by Xu et al. (2023) focused on the early detection of lung cancer using a novel SERS sensor composed of ZIF-8/4-ATP/Au/TiO₂ nanomaterial nanochannels [149]. Raman spectroscopy measurements were performed on seven types of aldehydes pertinent to lung cancer detection—such as benzaldehyde and formaldehyde—as well as various interfering gases, including hydrocarbons, alcohols, ketones, esters, nitriles, aromatic compounds, organic acids, and ammonia. Each Raman spectrum was composed of 571 data points ranging from 800 to 1800 cm⁻¹, with 638 spectra collected for each gas. PCA was employed for the dimensionality reduction of the data, while classification algorithms included KNN, RF, SVM, and DT models. All ML models demonstrated excellent predictive capabilities, achieving classification accuracies exceeding 96% in differentiating the seven aldehydes from the eight interfering substances. These studies underscore the effectiveness of integrating Raman spectroscopy with advanced ML techniques for non-invasive disease diagnosis via breath analysis. The high accuracy rates achieved highlight the potential of these methods for clinical applications in early detection and diagnosis. Table 8 presents the Raman spectroscopy-based breath research reviewed in this work, which focuses on the detection of lung and gastric cancers.

Table 8. Breath analysis studies that exploited Raman spectroscopy.

Author	Year	Application Domain	Breath Analysis Technique	Subjects	Feature Engineering	Machine Learning	Validation	Results
Xie et al. [148]	2024	LC and GC	SERS spectrum of exhaled breath in plasmonic metal-organic framework (PMN) film	49 HS, 22 LC and 8 GC (BS: 1780)	PCA, RF Classifier and Permutation Importances	Shallow ANN	Hold-out (80/20%)	89% Acc
Xu et al. [149]	2023	Detection of early LC	ZIF-8/4-ATP/Au/TiO ₂ NM-Based N anochannels SERS Sensor	For each gas, 638 Raman spectra were collected.	PCA	KNN, RF, SVM, and DT	Hold-out (80/20%)	Acc above 96%

3.3.3. Spectroscopy

Breath analysis has also been conducted via spectroscopic techniques to diagnose diseases, as demonstrated by two recent studies. The first study by Aslam et al. (2021) focused on classifying gastric cancer and detecting early stages of the disease [150]. The authors analyzed breath samples using a spectral range from 400 to 1500 nm. The study involved 200 spectra collected from 200 breath samples, including 55 EGC patients, 56 healthy individuals, and 89 advanced gastric cancer (AGC) patients. Each spectrum contained 1200 distinct values. The dataset was divided into training (70%), validation (15%), and testing (15%) sets. Multiple machine learning models were used, with DSAENN achieving an outstanding overall accuracy of 96.3% for gastric cancer classification, and an accuracy of 97.4% for early gastric cancer detection. In a second study by Nguyen et al. in 2023, the focus shifted to diagnosing lung cancer using a gap plasmonic film fabrication technique [151]. The authors of this work collected breath samples from 120 subjects, comprising 70 healthy participants and 50 lung cancer patients. The dataset contained 360 samples (three locations per subject), each represented by 7200 unique features. These features were derived from three RGB values multiplied by 12 color films from a multi-array biosensor across 200 time points. A CNN was employed for classification, achieving an average accuracy of 89.58% across the five-fold cross-validation. These studies demonstrate the effectiveness of integrating spectroscopy with machine learning techniques in accurately diagnosing diseases through breath analysis, underscoring the promise of non-invasive diagnostic methods in clinical settings. Table 9 presents the latest research that used spectroscopy to detect lung and gastric cancers through breath analysis.

Table 9. Breath analysis studies using Spectroscopy.

Author	Year	Application Domain	Breath Analysis Technique	Subjects	Feature Engineering	Machine Learning	Validation	Results
Nguyen et al. [151]	2023	LC	Gap Plasmonic Film Fabrication	70 HS and 50 LC (BS: 360)	-	CNN	Hold-out (80/20%) and 5-fold CV	89.58% averaged Acc for CNN with a 5-fold CV
Aslam et al. [150]	2021	GC diagnosis and early GC detection	Spectral region from 400 to 1500 nm	55 EGC, 56 HS, and 89 AGC (BS: 200)	-	DSSAENN	Hold-out (70/15/15%)	Gastric Cancer Classification: 96.3% Acc Early Gastric Cancer Detection: 97.4% Acc

3.4. Gas Chromatography

Gas chromatography is a widely used technique in breath analysis due to its high sensitivity, ability to provide an orthogonal analysis, extensive compound libraries, and capacity to detect VOCs associated with various diseases. This section examines two studies that utilized gas chromatography for disease diagnosis. Table 10 summarizes these studies, outlining their methods, ML approaches, and validation strategies. In the first study, Picciariello et al. investigated the use of an automated portable gas chromatography device to diagnose CRC [152]. They analyzed breath samples from 36 CRC patients (without metastases) and 32 healthy participants, using 100 different VOCs. For data processing,

they implemented PCA for feature engineering and LDA for classification, testing their model on 18 patients with CRC and 14 healthy controls. The results were promising: the method attained a specificity of 87.5% (correctly identifying healthy individuals), a sensitivity of 94.4% (correctly identifying patients with CRC), and an overall accuracy of 91.2%. In the second study, Zhou et al. examined a two-dimensional gas chromatography device for diagnosing acute respiratory distress syndrome (ARDS) [153]. They analyzed breath samples from 21 ARDS patients and 27 non-ARDS controls, detecting 97 VOC peaks. Similar to the first study, they employed PCA and LDA for feature extraction and classification, performing a 4-fold cross-validation to ensure the robustness of their model. The average classification accuracy across the four validation models was $85.3\% \pm 0.7\%$. These studies demonstrate that combining gas chromatography with ML techniques can accurately classify breath samples for disease diagnosis, highlighting the potential of these methods in developing non-invasive diagnostic technologies. Table 10 summarizes the latest research on gas chromatography-based breath analysis for detecting colorectal cancer and acute respiratory diseases.

Table 10. Breath analysis studies using gas chromatography.

Author	Year	Application Domain	Breath Analysis Technique	Subjects	Feature Engineering	Machine Learning	Validation	Results
Picciariello [152]	2024	Colorectal Cancer	Automated portable gas chromatography device	68 subjects: 36 patients (no metastases), 32 HS	PCA	LDA	Training set (18 CRC and 18 HC)/Testing set (18 CRC and 14 HC)	87.5% Spe, 94.4% Sen, 91.2% Acc
Zhou et al. [153]	2019	ARDS	Two-dimensional gas chromatography device	21 ARDS and 27 non-ARDS HS (BS: 85)	PCA	LDA	Training set (28 subjects)/ Testing set (20 subjects)/ 4-fold CV	87.1% Overall Acc, 94.1% PPV and 82.4% NPV

3.5. Summary of Findings

This scoping review analyzed 97 studies applying machine learning to breath analysis for disease diagnosis across respiratory (48%), metabolic (22%), and oncological (20%) conditions. Table 11 summarizes the reviewed studies by disease category, analytical technique, ML algorithms, validation approaches, and performance metrics. E-Nose platforms and spectrometric methods dominated the field, with traditional ML algorithms (SVM, RF) and emerging deep learning approaches achieving diagnostic accuracies of 85–98% (median AUC: 0.93).

Table 11. Summary of reviewed studies by disease category, analytical/sensing technology, ML algorithm, validation approach, and best reported performance.

Disease Category	Analytical/Sensing Technique	Typical Sample Size (N)	Common ML/DL Algorithms	Validation Strategy	Best Reported Performance	Representative References
Respiratory diseases (LC, COPD, Asthma, TB, COVID-19)	e-Nose (MOS, QMB), GC-MS, PTR-MS, SIFT-MS, HPPI-TOFMS	30–400	RF, SVM, XGBoost, CNN, LSTM	5-fold CV, LOOCV, hold-out	Acc = 90–98%; AUC = 0.93–0.99	Zhao 2021 [66]; Rivai 2024 [70]; Fu 2023 [108]
Metabolic disorders (Diabetes, obesity, NAFLD)	e-Nose, TD-GC-MS	40–200	SVM, RF, hybrid DL (SVM + CNN)	10-fold CV, hold-out	Acc = 93–98%; AUC \approx 0.95	Bhaskar 2023 [99]; Gudiño-Ochoa 2024 [57]
Oncological diseases (breast, colorectal, liver, gastric, prostate cancers)	GC-MS, SIFT-MS, HPPI-TOFMS, e-Nose	100–2000	RF, XGBoost, CNN	k-fold CV, external validation	Acc = 85–94%; AUC = 0.90–0.98	Zhang 2024 [113]; Poljaka 2023 [90]
Infectious diseases (tuberculosis, COVID-19)	HPPI-TOFMS, PTR-MS, e-Nose	70–500	RF, GBM, CNN	5-fold CV, hold-out	Acc = 88–96%; AUC \approx 0.96	Doğuç 2023 [60]; Roquencourt 2023 [104]

Table 11. Cont.

Disease Category	Analytical/Sensing Technique	Typical Sample Size (N)	Common ML/DL Algorithms	Validation Strategy	Best Reported Performance	Representative References
Neurological/psychiatric disorders (schizophrenia, MDD, Parkinson's)	PTR-MS, GC-MS	50–150	LR, BART, SVM	Forward selection, CV	Acc = 75–85%	Henning 2023 [117]
Others/mixed diseases (cystic fibrosis, pulmonary fibrosis)	PTR-TOF-MS, GC-MS	30–200	LASSO, RF, XGBoost	5-fold CV	AUC = 0.87–0.99	Mustafina 2024 [114]; Taylor 2024 [118]

4. Discussion

This scoping review examines the application of ML in breath analysis for disease diagnosis and prognosis, emphasizing its potential as a non-invasive diagnostic tool. The findings demonstrate a growing reliance on ML to process VOCs, with spectrometric and sensor-based techniques emerging as the most commonly used analytical approaches to date. Ensemble learning models (particularly RF and GBM) are often employed to enhance classification accuracy, while DL methods are increasingly used to manage complex breathomics data. Despite these advancements, several challenges remain, including the need for standardized breath analysis protocols, the limited generalizability of ML models due to small and homogeneous datasets, and the gap between experimental results and clinical implementation. The following sections examine these trends, discussing the latest technological innovations, methodological limitations, and the potential directions for future research.

Rise of ML in Breath Analysis: The temporal distribution of studies (Figure 2) reveals a sharp increase in the number of machine learning applications for breath analysis over the past decade, with a particularly pronounced rise from 2020 onward. The number of studies remained relatively stable between 2018 and 2020, averaging fewer than 10 publications per year, but surged in 2021, coinciding with the COVID-19 pandemic. This shift reflects the heightened global interest in respiratory disease diagnostics, as breath analysis gained traction as a potential screening tool for COVID-19. The respiratory system consistently dominates ML-driven breath analysis, accounting for over 50% of studies in recent years, with applications in lung cancer, COPD, asthma, and infectious disease diagnosis. However, the expansion of breathomics research into metabolic and gastrointestinal disorders has also been notable, with studies on diabetes, liver disease, and colorectal cancer increasing by approximately 30% from 2021 to 2024. In contrast, cardiovascular and neurological diseases remain underrepresented, likely due to the lack of well-established breath biomarkers for these conditions and a historical reliance on more traditional diagnostic methods such as imaging and blood tests. The projection for 2025 suggests a continued growth in established research areas, while preliminary investigations into dermatological and autoimmune conditions signal the potential emergence of new research directions. These findings underscore the evolving landscape of breath-based diagnostics, where technological advancements and global health priorities continue to shape the research focus.

Trends in Breath Analysis Techniques: The rapid development of breath-based diagnostic technologies has led to a diverse landscape of analytical methods, with spectrometric techniques and sensor-based approaches dominating most disease categories (Figure 3). Sensors have emerged as the most widely used category, demonstrating a strong connection to respiratory diseases, while also contributing to other areas, including the endocrine, urinary, and digestive systems. This widespread adoption likely arises from their real-time detection capabilities, affordability, and ease of integration into portable devices. Spectrometric techniques, although heavily associated with respiratory diseases, also play a significant role in the detection of digestive and endocrine disorders, indicating their capability to

detect a broad spectrum of VOCs, relevant to metabolic and systemic diseases. In contrast, gas chromatography is the least utilized technique, focusing mainly on colorectal cancer detection, with minor contributions to respiratory disease diagnostics. These patterns highlight the tailored nature of technique selection, where disease-specific biomarker profiles and analytical precision guide the preferred methodology. Moving forward, integrating multiple breath analysis techniques—leveraging the broad applicability of sensors, the chemical specificity of spectrometry, and the high-resolution capabilities of GC—could lead to more robust and comprehensive breath-based diagnostic solutions.

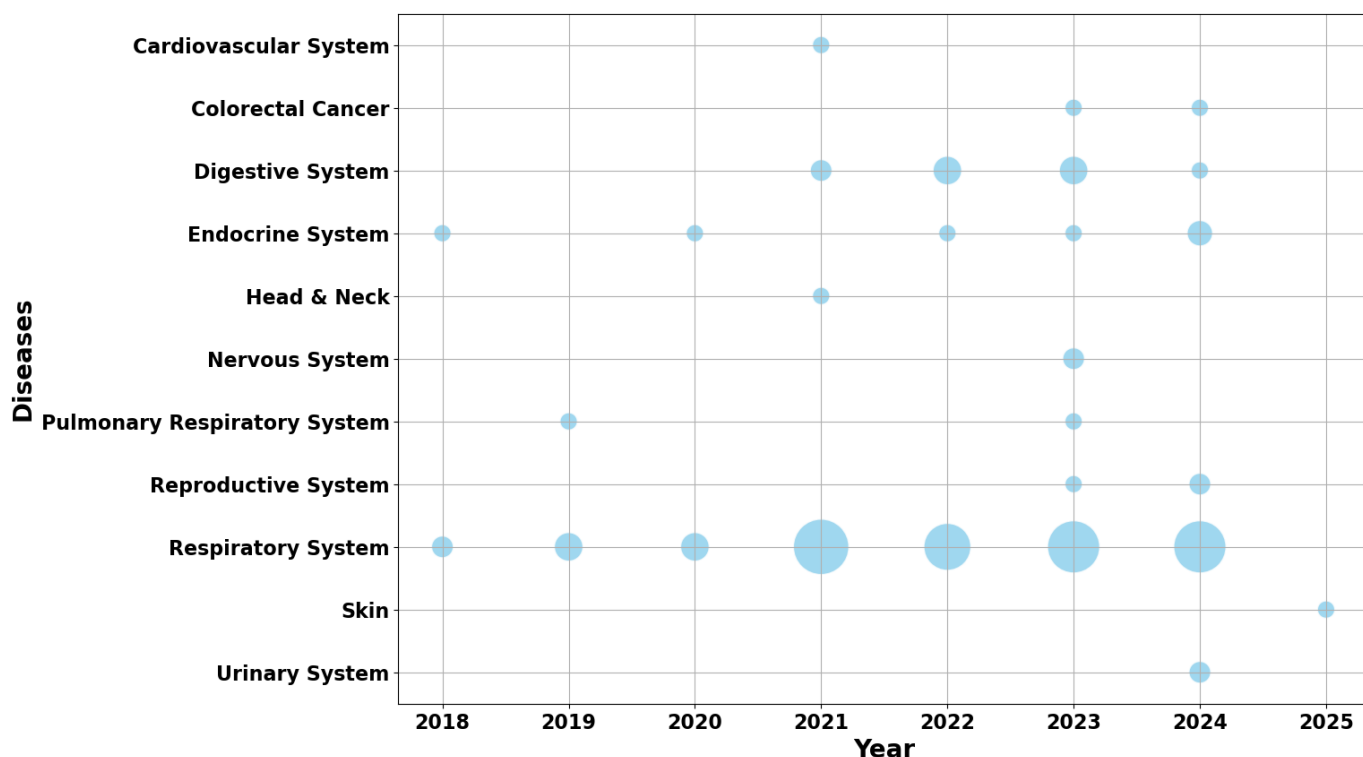


Figure 2. Annual Distribution of Studies by Disease Category.

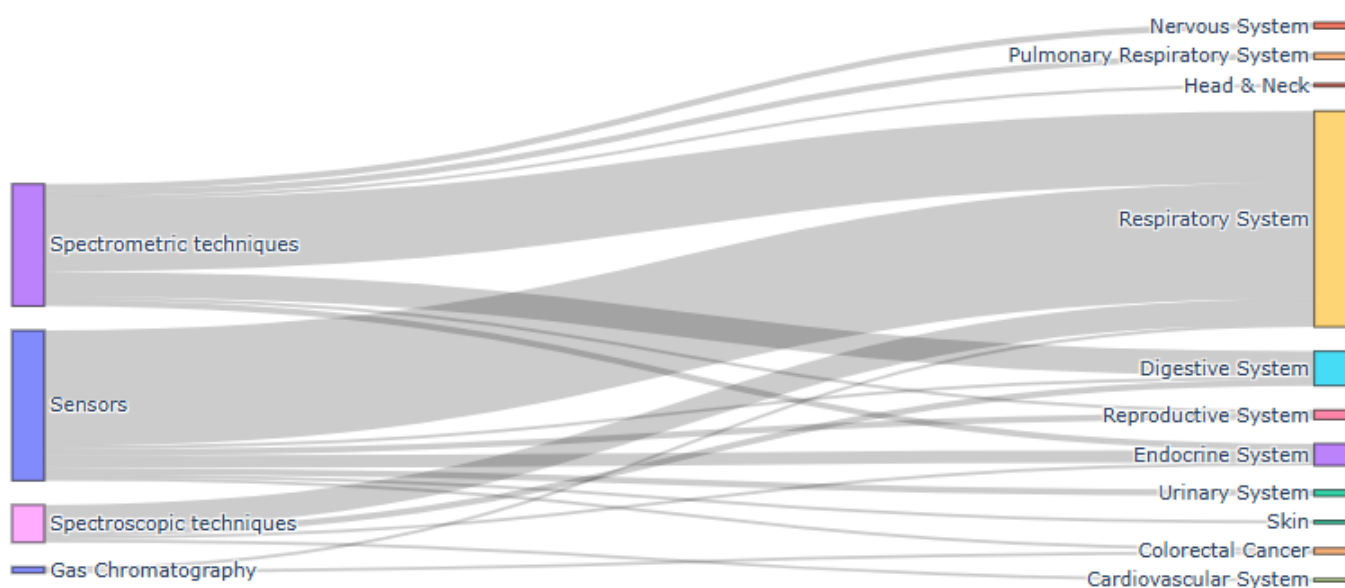


Figure 3. Breath Analysis Techniques for Disease Detection.

ML Model Preferences: The trends in ML applications for disease classification and prediction using breath analysis reveal a clear preference for traditional ML models and ensemble methods, along with a growing shift toward deep learning and hybrid approaches. As techniques advance and breathomics data become more complex, researchers increasingly turn to sophisticated modeling strategies to enhance predictive accuracy, model robustness, and clinical applicability. Figure 4 illustrates the distribution of ML models across various diseases, with the respiratory system emerging as the most heavily studied category. Traditional ML models, such as SVM, RF, KNN, DT, and LR, dominate applications for respiratory diseases (35 studies), followed by ensemble and boosting techniques, including XGBoost, AdaBoost, gradient boosting machines, and LightGBM (26 studies). These methods are widely utilized for their robustness in handling high-dimensional VOC datasets, effective feature selection, and strong generalization performance. In contrast, digestive and endocrine disorders exhibit a more varied but relatively limited application of ML models, incorporating NNs, probabilistic models, and traditional approaches in smaller numbers. This suggests an exploratory phase in these domains, where different modeling techniques are being tested, but where no dominant methodology has yet emerged. Notably, unsupervised learning approaches are underrepresented, highlighting a potentially underutilized strategy in exploratory biomarker discovery. Given the potential of unsupervised methods to identify hidden patterns in high-dimensional VOC data, their limited representation indicates a research gap that should be addressed in future studies.

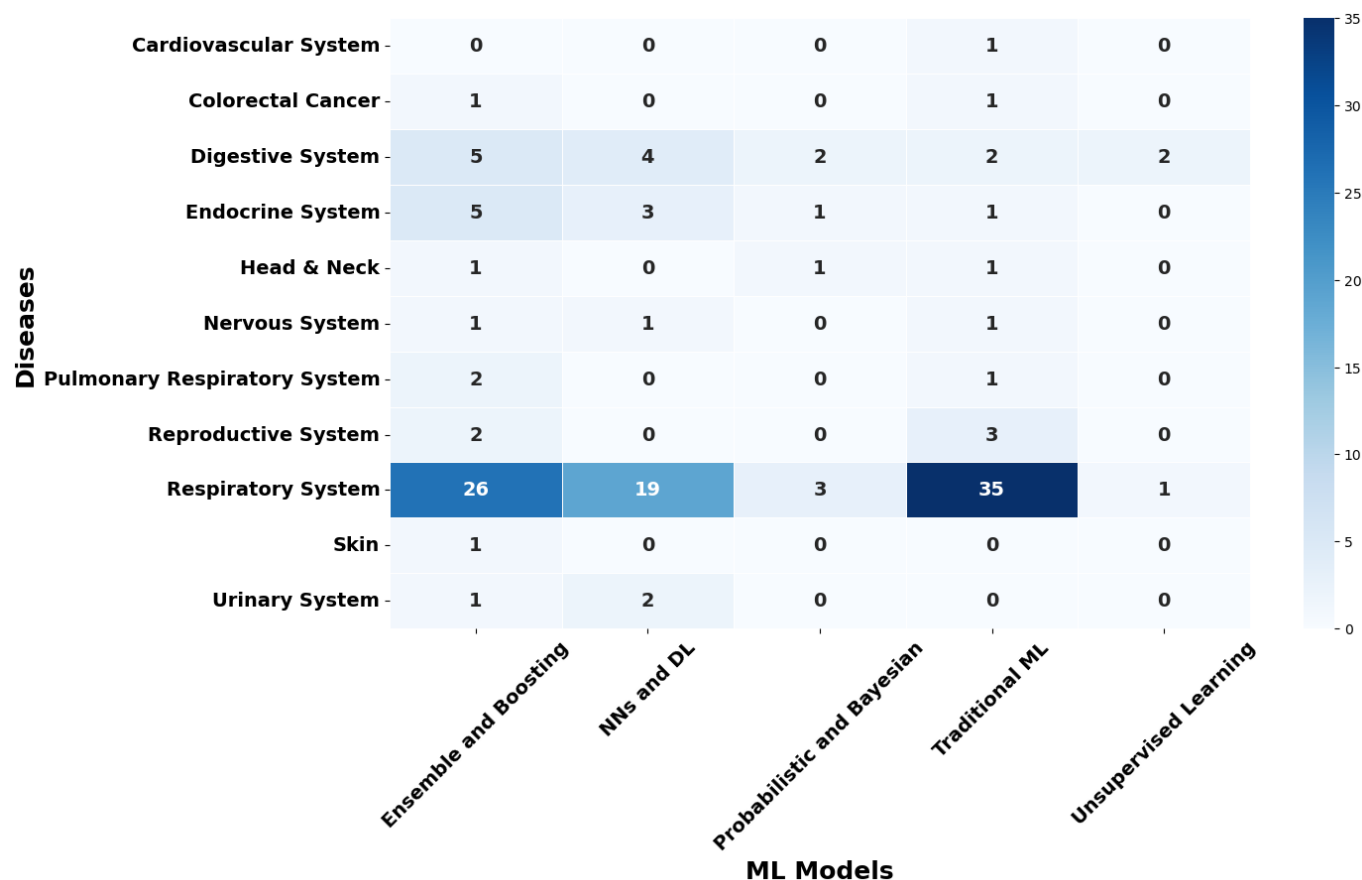


Figure 4. Distribution of Machine Learning Models Across Disease Categories in Breath Analysis.

A shift towards hybrid and deep learning models is reshaping ML applications in breathomics. DL architectures, such as CNNs, are increasingly being applied to respiratory diseases (asthma, COPD, lung cancer, COVID-19, and tuberculosis) due to their ability to capture complex spatial and temporal patterns in VOC profiles. These models, often paired

with traditional classifiers such as RF and SVM, offer enhanced accuracy and robustness. Hybrid models that integrate feature extraction methods like CNNs with ensemble classifiers such as RF, XGBoost, and GBM have proven highly effective in improving predictive performance. Stacking models (where the output of one algorithm is used as the input for another) have facilitated the development of sophisticated and accurate predictive systems, particularly in electronic noses, spectroscopic, and spectrometric techniques, where the complexity of breath data necessitates advanced modeling strategies. Moreover, transfer learning techniques and hybrid architectures have been observed in more recent studies, particularly within spectrometric applications, indicating a shift towards more sophisticated model development to handle complex datasets.

In most DL-based studies, raw spectral or sensor array signals are preprocessed using normalization and scaling, then reshaped into 1D or 2D matrices suitable for convolutional processing. CNNs extract spatial or correlation-based features from spectra or sensor responses, while LSTM and GRU models capture temporal dependencies from time-series breath data. Recent advances include hybrid models, such as CNN-XGBoost and CNN-Autoencoder combinations, that leverage both learned representations and structured feature-based classification. Transfer learning from pretrained image or signal models (e.g., ResNet and VGG) has also been applied to breathomics, improving performance in small datasets.

Across numerous disease categories, specific trends in ML model preferences have been observed. For respiratory diseases such as asthma, COPD, lung cancer, COVID-19, and pulmonary tuberculosis, deep learning models such as CNN and LSTM are increasingly favored for pattern recognition in high-dimensional datasets. In cancer detection, encompassing lung, colorectal, breast, and prostate cancers, ensemble methods such as RF, XGBoost, LightGBM, and LR dominate. In metabolic disorders such as diabetes, liver disease, and insulin resistance, studies show a growing preference for hybrid ML techniques, with deep learning approaches including CNN-XGBoost combinations commonly employed, particularly for handling complex spectrometric data. Similarly, in the field of liver and gastrointestinal diseases (cirrhosis, HCC, and gastric cancer), ensemble models, especially XGBoost, RF, and LDA, are frequently utilized.

Despite these advancements, some ML techniques remain underutilized. Probabilistic and Bayesian models are seldom applied in breath analysis, despite their potential to offer valuable uncertainty quantification for clinical decision-making. Similarly, unsupervised learning methods, such as clustering and anomaly detection, remain largely unexplored, despite their potential for identifying novel biomarker patterns without the need for labeled datasets. Given the inherent complexity of breathomics data, integrating these underrepresented ML methodologies could unlock new insights and enhance model interpretability in future studies. The evolution of ML techniques in breath analysis reflects a shift towards more complex and integrated modeling approaches. While traditional ML methods continue to serve as the foundation for disease classification, future research should focus on expanding hybrid models, DL applications, and underutilized probabilistic and unsupervised learning strategies in order to improve the reliability, scalability, and interpretability of AI-driven breath diagnostics.

Sample Size Analysis: Sample size is a critical factor in determining the robustness, reliability, and generalizability of ML-driven breath analysis models. Figure 5 illustrates the distribution of sample sizes in the reviewed studies, revealing a strong skew toward smaller datasets, with most studies falling into the first bin (fewer than 40 participants). Furthermore, the vast majority of studies incorporate fewer than 100 subjects in total across all classes, underscoring the limited scope of data used to train and validate ML models. The predominance of small-scale studies suggests that much of the current research remains at the pilot or exploratory stage, focusing on the initial validation of breath analysis

techniques in controlled environments rather than in the large-scale clinical setting. While a few studies incorporate larger cohorts ranging from 500 to 2000 participants, these remain exceptions rather than the norm, highlighting an ongoing challenge in scaling breathomics research to real-world applications. The reliance on small datasets raises concerns about model overfitting, poor generalizability, and potential biases, as ML algorithms trained on limited and homogeneous data may struggle to perform reliably across diverse populations. Overcoming these limitations will require multi-center collaborations, standardized data collection protocols, and larger, more diverse cohorts to ensure breath-based ML models transition from promising experimental tools to clinically viable diagnostic solutions.

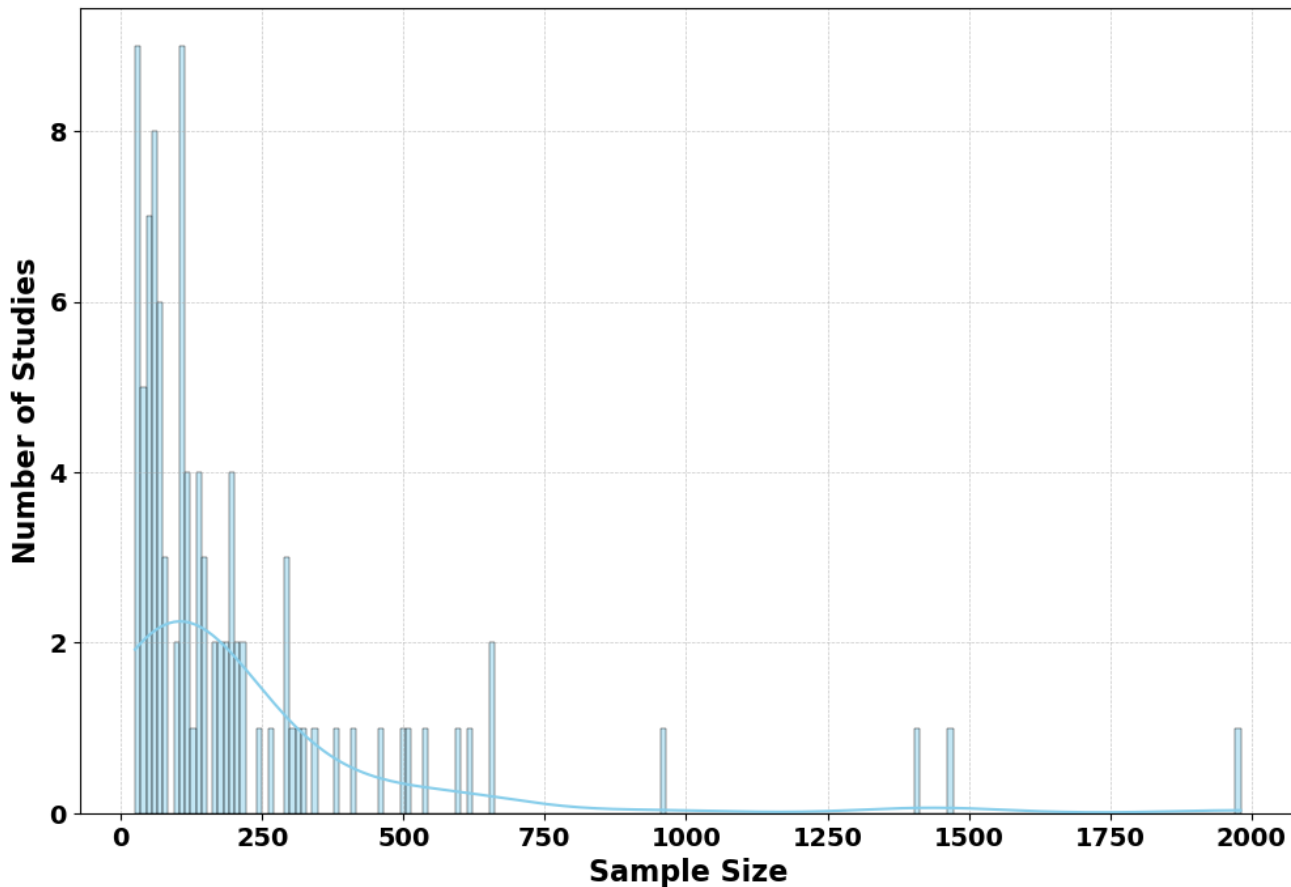


Figure 5. Distribution of Sampled Employed Studies.

Alignment of Breath Analysis Techniques with ML Models: Building on the challenges of sample size limitations, the interaction between breath analysis techniques and ML models underscores the importance of methodological alignment in breath metabolomics research (Figure 6). Spectrometric techniques and sensors dominate the analytical landscape, primarily employing ensemble and boosting approaches (27 and 15 studies, respectively) alongside traditional ML models (18 and 19 studies, respectively). This preference reflects the ability of these ML models to handle the high variability and complex data structures characteristic of spectrometric and sensor-based analyses, where large feature sets and intricate VOC patterns demand advanced feature selection and classification strategies. In contrast, gas chromatography exhibits minimal integration with ML, which is likely due to its narrow application scope and the complexity of VOC separation processes that may not always require advanced computational modeling. A particularly noteworthy observation is the limited use of probabilistic and Bayesian models across all techniques, despite their potential for uncertainty quantification and improved decision-making in diagnostic pre-

dictions. This underutilization suggests an area for methodological improvement, where Bayesian inference could enhance the interpretability and reliability of ML-driven breath diagnostics. Overall, these findings highlight the importance of selecting ML strategies that align with the specific data characteristics of each breath analysis technique, ensuring optimal diagnostic performance and clinical applicability. Future research should explore hybrid modeling approaches that combine the strengths of different ML paradigms to enhance robustness and predictive confidence in breath-based disease detection.

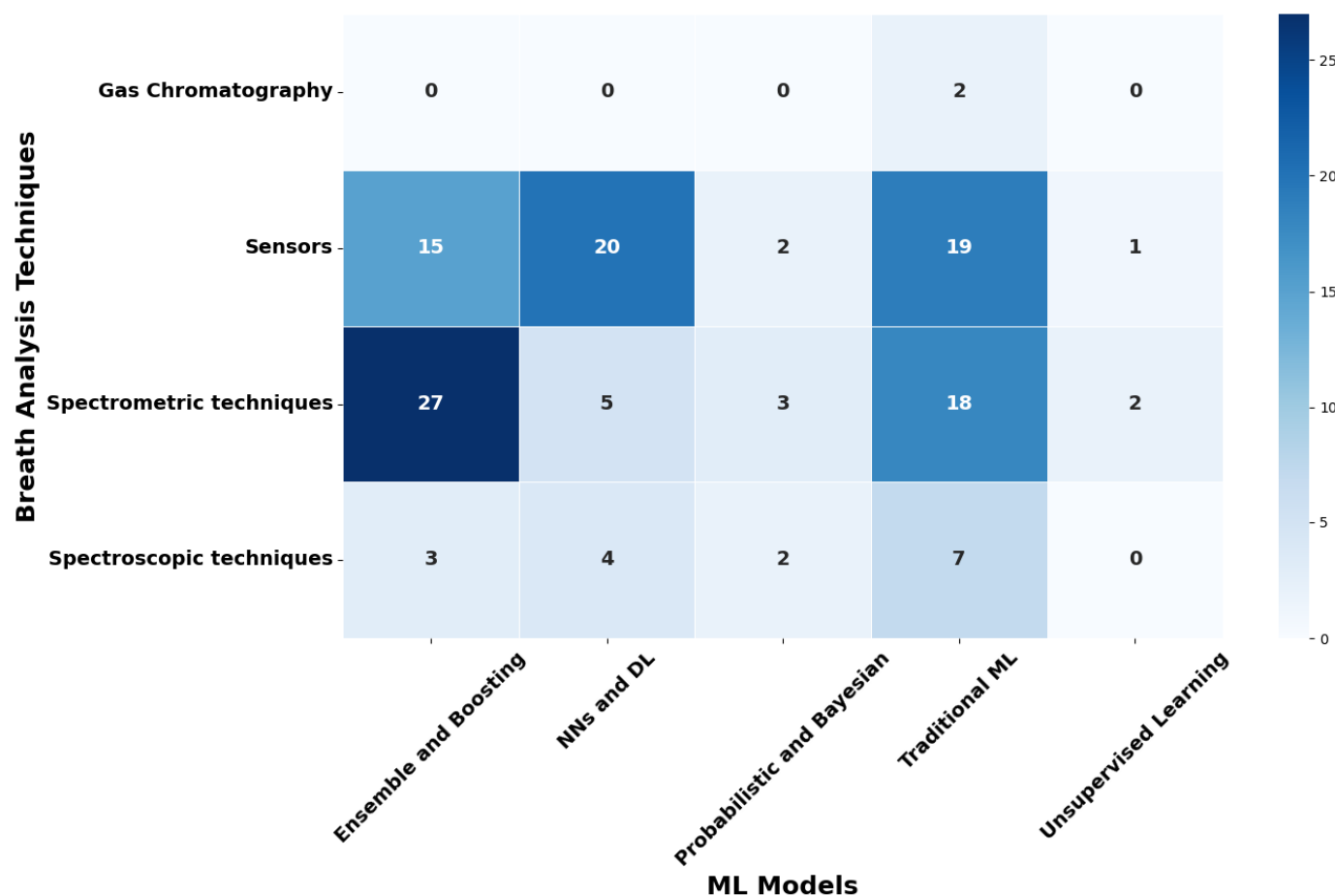


Figure 6. Alignment of Breath Analysis Techniques with Machine Learning Models.

The Role of Feature Engineering: Feature selection and dimensionality reduction are crucial for managing the high-dimensional nature of breathomics datasets, ensuring enhanced model performance, interpretability, and computational efficiency. PCA is the most commonly used technique, appearing in 73.8% of studies, as it effectively preserves variance while reducing the complexity of the feature space. However, alternative machine learning-based feature selection methods account for 26.2% of the approaches, suggesting a shift toward data-driven feature selection strategies. These include Boruta feature selection (Boruta FS), ReliefF, RFE, genetic algorithms, and SHAP-based ranking, all of which provide more targeted and flexible biomarker identification strategies in comparison to traditional dimensionality reduction techniques. Additionally, ensemble-based feature selection methods—such as those integrating RF, XGBoost, and LR—have been utilized to improve model robustness and to ensure the relevance of selected VOC features in disease classification. Advanced feature engineering techniques are also influencing early detection efforts in specific disease domains. In liver and gastrointestinal diseases, such as cirrhosis, HCC, and GC, ensemble models such as XGBoost, RF, and LDA often combine hybrid

feature selection pipelines to enhance predictive accuracy. Techniques such as isolation forest algorithms and hybrid PCA-SHAP models have emerged as promising solutions for improving early-stage disease detection by filtering out irrelevant features and emphasizing key biomarkers.

Validation: Strategies for validation were essential in evaluating the reliability, robustness, and generalizability of ML models in breathomics research. Most studies utilized 5-fold and 10-fold CV techniques, regarded as gold-standard methods for reducing overfitting and ensuring consistent model performance across various data subsets. These techniques offered reliable error estimation while remaining computationally efficient, leading to widespread use in different ML applications related to breath analysis. In cases with limited sample sizes, especially in spectrometric analyses, LOOCV was often preferred to maximize data utilization and to avoid performance inflation linked to small dataset bias. While LOOCV was beneficial for highly constrained datasets, it incurred higher computational costs and greater variance in model estimates, making it less suitable for larger studies. Hold-out validation methods, such as 80/20% and 70/30% splits, were frequently employed in deep learning contexts where extensive training data was necessary. These methods enabled models to learn from a significant portion of the data while setting aside an independent test set for assessing generalization performance. Hold-out validation could, however, be prone to partitioning biases, particularly with smaller datasets (unless used alongside multiple random splits or stratified sampling techniques). Stratified validation was also adopted in several studies to ensure balanced disease class representation within the training and testing datasets. This was crucial for handling imbalanced datasets, where some disease conditions were underrepresented, which could inherently skew model predictions and decrease sensitivity for rare conditions. Stratified CV or class-weight adjustments aided in reducing bias and enhancing model performance across many disease categories.

VOC-Disease Insights: The relationship between volatile organic compounds and diseases (Figure 7) reveals both disease-specific biomarkers and multi-system indicators that guide diagnostic development. Several VOCs demonstrate strong disease specificity: acetone shows the most robust association with diabetes (8 studies), reflecting increased ketone body production during hyperglycemia; nitric oxide exhibits pronounced specificity for asthma (6 studies), consistent with airway inflammation; and aromatic compounds—benzene, toluene, and ethylbenzene—consistently associate with lung cancer (5 studies each), likely reflecting oxidative stress and altered metabolism in malignant tissue. In contrast, some VOCs serve as multi-disease indicators: acetone appears in diabetes, lung cancer, and kidney disease, suggesting its role as a general metabolic stress marker, while ammonia elevation occurs across kidney disease and lung cancer, reflecting disrupted nitrogen metabolism. The frequent use of complex VOC mixture patterns for COVID-19 (12 studies) and COPD (8 studies) indicates that multivariate signatures often outperform single biomarkers, explaining the success of machine learning approaches. The three-layer structure connecting VOCs to diseases to body systems demonstrates breath analysis captures both organ-specific pathology and systemic disruption: while respiratory diseases dominate (65 connections), detection of metabolic (16 connections), hepatic (19 connections), renal (7 connections), and neurological disorders (4 connections) validates breath as a systemic diagnostic modality. These patterns suggest optimal strategies should combine disease-specific VOCs for targeted screening with VOC pattern recognition for differential diagnosis of complex conditions.

Limitations: This scoping review has several inherent limitations. First, certain methodological decisions, such as the choice of databases, search keywords, and inclusion/exclusion criteria, were necessarily subjective and may have resulted in the omission of relevant studies. Second, heterogeneity among the included studies, such as differences in breath sampling techniques, disease cohorts, analytical platforms, and ML validation

methods, restricted direct comparability and the ability to perform a quantitative synthesis. Third, publication bias might favor studies that report positive or high-performing outcomes, potentially exaggerating the apparent success of ML models. Finally, although the review includes studies published up to February 2025, rapid advancements in AI and sensor technologies may have led to new developments not yet reflected in this analysis.

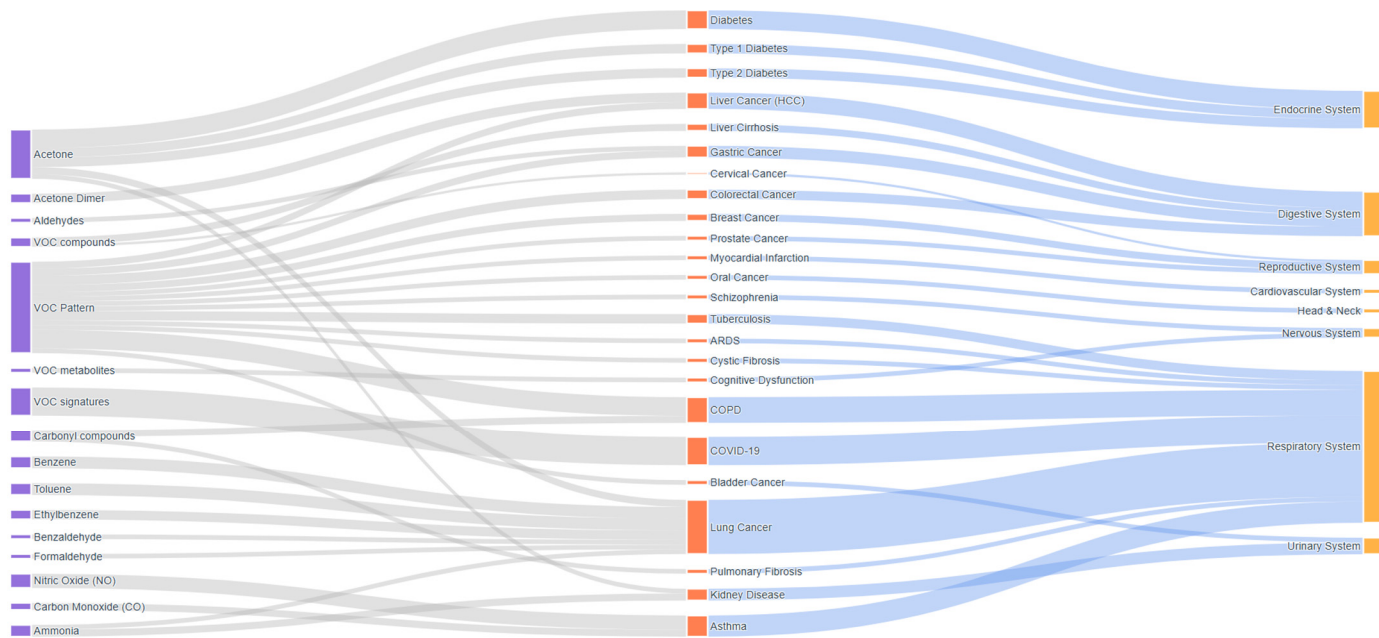


Figure 7. Volatile Organic Compound Biomarkers Linked to Diseases and Body Systems in Breath Analysis Studies.

Unexplored areas and future directions: Despite significant advancements in ML applications for breath VOC analysis, several critical areas remain underexplored, particularly in explainability, standardization, and integration with clinical workflows. Explainability techniques, which are essential for building clinical trust in AI-driven diagnostics, were explicitly addressed in only three out of 97 studies. Among these, one utilized case-based reasoning for interpretability, while another employed SHAP to assess feature contributions to model predictions. The limited use of explainability frameworks underscores a gap in making ML models transparent, interpretable, and actionable for clinical decision-making. Another key limitation is the lack of standardization in data collection, preprocessing, and model evaluation. Breathomics datasets vary significantly in terms of sampling methods, VOC profiling techniques, and reference standards, making cross-study comparisons and model reproducibility challenging. While RF and SVM models have proven effective for handling high-dimensional datasets, their widespread use has not been accompanied by sufficient benchmarking against deep learning architectures, hybrid models, or probabilistic frameworks. Similarly, while PCA remains a dominant approach for dimensionality reduction, alternative data-driven selection techniques (e.g., genetic algorithms, ReliefF, and ensemble-based feature selection) have been underutilized in breath analysis.

The integration of hybrid and ensemble approaches with deep learning remains another underexplored frontier in breathomics research. While deep learning models have demonstrated potential in capturing complex non-linear relationships within VOC datasets, they remain underutilized in combination with traditional ML frameworks. By integrating ensemble learning techniques with deep neural networks, transfer learning or generative models could enhance both predictive accuracy and biomarker discovery. Balancing model complexity with clinical interpretability remains one of the most pressing

challenges in ML-driven breath analysis. High-performing models often act as black boxes, limiting their practical adoption in medical diagnostics. As the field evolves, future research must prioritize the incorporation of explainability tools, standardization frameworks, and benchmarking studies to validate ML models across diverse clinical settings. The continued refinement of methodologies coupled with advancements in feature selection, transfer learning, and uncertainty quantification holds great potential for enhancing the diagnostic and prognostic capabilities of breathomics. These developments could bridge the gap between computational models and real-world clinical applications, ultimately advancing precision medicine and improving patient outcomes.

Several studies from the reviewed literature exemplify the successful application of ML-based breath analysis in real-world or clinically relevant contexts. For instance, Zhang et al. (2024) conducted a large-scale, multi-center study using HPPI-TOF-MS for breast cancer detection, integrating RF and XGBoost models trained on over 1900 breath samples collected across different hospitals [113]. The resulting models achieved a sensitivity of 85.9% and a specificity of 90.4%, demonstrating strong generalizability across diverse populations. Similarly, Fu et al. (2023) reported high diagnostic accuracy ($AUC = 0.975$) for tuberculosis detection using RF models trained on HPPI-TOF-MS data, validated on an independent external cohort [108]. Both studies demonstrate how larger, heterogeneous datasets and robust validation strategies can significantly enhance model reliability and clinical relevance. These examples underscore the importance of multi-center collaborations and standardized analytical pipelines in ensuring that ML-driven breath diagnostics are not only accurate but also reproducible and transferable across various healthcare settings.

The findings of this scoping review indicate that ensemble and DL methods (e.g., RF, XGBoost, CNN, and LSTM) consistently outperform traditional algorithms in terms of diagnostic accuracy for breath-based disease detection. However, interpretability remains a key barrier to clinical translation. Based on these insights, our ongoing work emphasizes the integration of explainable AI techniques—such as SHAP and attention mechanisms—into breathomics modeling to improve transparency while maintaining predictive performance. Additionally, multi-modal data fusion (combining VOC profiles with demographic or imaging data) is being explored as a strategy to enhance diagnostic robustness and early disease detection.

Recent advances in explainable artificial intelligence (XAI) have begun to address the “black-box” nature of complex ML and DL models in breathomics. Techniques such as SHAP and LIME (Local Interpretable Model-Agnostic Explanations) allow for quantification of individual feature contributions, helping to identify which volatile organic compounds (VOCs) most influence diagnostic predictions. These methods enhance model transparency and support biological interpretability by linking computational outputs with clinically meaningful biomarkers. For imaging- or signal-based DL architectures, visualization tools such as Grad-CAM (Gradient-weighted Class Activation Mapping) have been employed to highlight the spectral or sensor regions most responsible for classification, further bridging the gap between AI predictions and pathophysiological insights. Beyond interpretability, robust validation practices are essential to ensure reproducibility and clinical trust. Although internal cross-validation methods (e.g., k-fold or leave-one-out) are widely applied, only a minority of studies incorporate external validation or multi-center datasets, limiting generalizability across populations and devices. Future studies should adopt standardized validation protocols, include heterogeneous patient cohorts, and pursue collaborative, multi-institutional datasets to improve robustness and clinical applicability of AI-driven breath diagnostics.

5. Conclusions

Machine learning has become a powerful tool in breathomics, enabling non-invasive disease diagnosis and prognosis through the analysis of VOCs. This review demonstrates that traditional algorithms such as support vector machines and random forests remain dominant, while ensemble and deep learning models are increasingly adopted for their superior handling of complex breath data. The integration of ML with analytical and sensing technologies, such as GC–MS, PTR–MS, SIFT–MS, and electronic noses, has significantly improved diagnostic accuracy and biomarker discovery.

However, several challenges persist, including the lack of standardized sampling protocols, limited interpretability of complex models, and the need for larger, multi-center datasets for external validation. To address these gaps, future research should focus on developing explainable AI frameworks, harmonized data standards, and collaborative studies to enhance clinical reliability. Establishing standardized benchmark datasets will be essential to facilitate model comparison and reproducibility, while the implementation of federated learning frameworks can enable privacy-preserving collaboration across institutions and provide access to larger, more diverse datasets. Furthermore, integrating breathomics with other omics layers, such as genomics, proteomics, and metabolomics, could unlock comprehensive, multi-dimensional insights for precision diagnostics and personalized medicine.

Funding: The research leading to this review paper has received funding from the VOCORDER project, which is co-funded by the European Union under grant agreement 101115442 and the State Secretariat for Education, Research, and Innovation (SERI), REF-1131-52304/SBFI-Nr.23.00369.

Institutional Review Board Statement: Not applicable.

Informed Consent Statement: Not applicable.

Data Availability Statement: No new data were created or analyzed in this study.

Conflicts of Interest: Authors Christos Kokkotis, Serafeim Moustakidis were employed by the company AIDEAS OÜ. The remaining authors declare that the research was conducted in the absence of any commercial or financial relationships that could be construed as a potential conflict of interest.

References

- Devillier, P.; Salvator, H.; Naline, E.; Couderc, L.-J.; Grassin-Delyle, S. Metabolomics in the Diagnosis and Pharmacotherapy of Lung Diseases. *Curr. Pharm. Des.* **2017**, *23*, 2050–2059. [[CrossRef](#)]
- Giannoukos, S.; Brkić, B.; Taylor, S.; France, N. Monitoring of Human Chemical Signatures Using Membrane Inlet Mass Spectrometry. *Anal. Chem.* **2014**, *86*, 1106–1114. [[CrossRef](#)]
- Giannoukos, S.; Brkić, B.; Taylor, S.; France, N. Membrane Inlet Mass Spectrometry for Homeland Security and Forensic Applications. *J. Am. Soc. Mass Spectrom.* **2014**, *26*, 231–239. [[CrossRef](#)]
- Giannoukos, S.; Agapiou, A.; Brkić, B.; Taylor, S. Volatolomics: A Broad Area of Experimentation. *J. Chromatogr. B* **2019**, *1105*, 136–147. [[CrossRef](#)]
- Giannoukos, S.; Agapiou, A.; Taylor, S. Advances in Chemical Sensing Technologies for VOCs in Breath for Security/Threat Assessment, Illicit Drug Detection, and Human Trafficking Activity. *J. Breath Res.* **2018**, *12*, 027106. [[CrossRef](#)]
- Chow, K.K.; Short, M.; Zeng, H. A Comparison of Spectroscopic Techniques for Human Breath Analysis. *Biomed. Spectrosc. Imaging* **2012**, *1*, 339–353. [[CrossRef](#)]
- Gresham, G. ClinicalTrials.Gov. In *Principles and Practice of Clinical Trials*; Piantadosi, S., Meinert, C.L., Eds.; Springer International Publishing: Cham, Switzerland, 2022; pp. 479–495, ISBN 978-3-319-52636-2.
- Cooks, R.G.; Ouyang, Z.; Takats, Z.; Wiseman, J.M. Ambient Mass Spectrometry. *Science* **2006**, *311*, 1566–1570. [[CrossRef](#)] [[PubMed](#)]
- Amann, A.; de Lacy Costello, B.; Miekisch, W.; Schubert, J.; Buszewski, B.; Pleil, J.; Ratcliffe, N.; Risby, T. The Human Volatileome: Volatile Organic Compounds (VOCs) in Exhaled Breath, Skin Emanations, Urine, Feces and Saliva. *J. Breath Res.* **2014**, *8*, 034001. [[CrossRef](#)] [[PubMed](#)]

10. Vishinkin, R.; Haick, H. Nanoscale Sensor Technologies for Disease Detection via Volatolomics. *Small* **2015**, *11*, 6142–6164. [[CrossRef](#)]
11. Broza, Y.Y.; Mochalski, P.; Ruzsanyi, V.; Amann, A.; Haick, H. Hybrid Volatolomics and Disease Detection. *Angew. Chem. Int. Ed.* **2015**, *54*, 11036–11048. [[CrossRef](#)] [[PubMed](#)]
12. Kaufman, E.; Lamster, I.B. The Diagnostic Applications of Saliva—A Review. *Crit. Rev. Oral Biol. Med.* **2002**, *13*, 197–212. [[CrossRef](#)]
13. Soini, H.A.; Klouckova, I.; Wiesler, D.; Oberzaucher, E.; Grammer, K.; Dixon, S.J.; Xu, Y.; Brereton, R.G.; Penn, D.J.; Novotny, M.V. Analysis of Volatile Organic Compounds in Human Saliva by a Static Sorptive Extraction Method and Gas Chromatography-Mass Spectrometry. *J. Chem. Ecol.* **2010**, *36*, 1035–1042. [[CrossRef](#)]
14. Fuchsmaier, P.; Stern, M.T.; Bischoff, P.; Badertscher, R.; Breme, K.; Walther, B. Development and Performance Evaluation of a Novel Dynamic Headspace Vacuum Transfer “In Trap” Extraction Method for Volatile Compounds and Comparison with Headspace Solid-Phase Microextraction and Headspace in-Tube Extraction. *J. Chromatogr. A* **2019**, *1601*, 60–70. [[CrossRef](#)]
15. Amann, A.; Poupart, G.; Telser, S.; Ledochowski, M.; Schmid, A.; Mechtcheriakov, S. Applications of Breath Gas Analysis in Medicine. *Int. J. Mass Spectrom.* **2004**, *239*, 227–233. [[CrossRef](#)]
16. Anderson, J.C. Measuring Breath Acetone for Monitoring Fat Loss. *Obesity* **2015**, *23*, 2327–2334. [[CrossRef](#)] [[PubMed](#)]
17. Giannoukos, S.; Brkić, B.; Taylor, S.; Marshall, A.; Verbeck, G.F. Chemical Sniffing Instrumentation for Security Applications. *Chem. Rev.* **2016**, *116*, 8146–8172. [[CrossRef](#)] [[PubMed](#)]
18. Vautz, W.; Slodzynski, R.; Hariharan, C.; Seifert, L.; Nolte, J.; Fobbe, R.; Sielemann, S.; Lao, B.C.; Huo, R.; Thomas, C.P. Detection of Metabolites of Trapped Humans Using Ion Mobility Spectrometry Coupled with Gas Chromatography. *Anal. Chem.* **2013**, *85*, 2135–2142. [[CrossRef](#)] [[PubMed](#)]
19. Pleil, J.; Risby, T.; Herbig, J. Breath Biomonitoring in National Security Assessment, Forensic THC Testing, Biomedical Technology and Quality Assurance Applications: Report from PittCon 2016. *J. Breath Res.* **2016**, *10*, 029001. [[CrossRef](#)]
20. Beck, O.; Sandqvist, S.; Dubbelboer, I.; Franck, J. Detection of Δ9-Tetrahydrocannabinol in Exhaled Breath Collected from Cannabis Users. *J. Anal. Toxicol.* **2011**, *35*, 541–544. [[CrossRef](#)]
21. Agapiou, A.; Amann, A.; Mochalski, P.; Statheropoulos, M.; Thomas, C.L.P. Trace Detection of Endogenous Human Volatile Organic Compounds for Search, Rescue and Emergency Applications. *TrAC Trends Anal. Chem.* **2015**, *66*, 158–175. [[CrossRef](#)]
22. Costanzo, M.T.; Boock, J.J.; Kemperman, R.H.; Wei, M.S.; Beekman, C.R.; Yost, R.A. Portable FAIMS: Applications and Future Perspectives. *Int. J. Mass Spectrom.* **2017**, *422*, 188–196. [[CrossRef](#)]
23. Wang, C.; Sahay, P. Breath Analysis Using Laser Spectroscopic Techniques: Breath Biomarkers, Spectral Fingerprints, and Detection Limits. *Sensors* **2009**, *9*, 8230–8262. [[CrossRef](#)]
24. McCurdy, M.R.; Bakirkin, Y.; Wysocki, G.; Lewicki, R.; Tittel, F.K. Recent Advances of Laser-Spectroscopy-Based Techniques for Applications in Breath Analysis. *J. Breath Res.* **2007**, *1*, 014001. [[CrossRef](#)]
25. Mochalski, P.; Wiesenhofer, H.; Allers, M.; Zimmermann, S.; Güntner, A.T.; Pineau, N.J.; Lederer, W.; Agapiou, A.; Mayhew, C.A.; Ruzsanyi, V. Monitoring of Selected Skin-and Breath-Borne Volatile Organic Compounds Emitted from the Human Body Using Gas Chromatography Ion Mobility Spectrometry (GC-IMS). *J. Chromatogr. B* **2018**, *1076*, 29–34. [[CrossRef](#)]
26. Bouhlel, J.; Bouveresse, D.J.-R.; Abouelkaram, S.; Baéza, E.; Jondreville, C.; Travel, A.; Ratel, J.; Engel, E.; Rutledge, D.N. Comparison of Common Components Analysis with Principal Components Analysis and Independent Components Analysis: Application to SPME-GC-MS Volatolomic Signatures. *Talanta* **2018**, *178*, 854–863. [[CrossRef](#)] [[PubMed](#)]
27. Curran, A.M.; Rabin, S.I.; Prada, P.A.; Furton, K.G. Comparison of the Volatile Organic Compounds Present in Human Odor Using SPME-GC/MS. *J. Chem. Ecol.* **2005**, *31*, 1607–1619. [[CrossRef](#)] [[PubMed](#)]
28. Phillips, M.; Cataneo, R.N.; Chaturvedi, A.; Kaplan, P.D.; Libardoni, M.; Mundada, M.; Patel, U.; Zhang, X. Detection of an Extended Human Volatome with Comprehensive Two-Dimensional Gas Chromatography Time-of-Flight Mass Spectrometry. *PLoS ONE* **2013**, *8*, e75274. [[CrossRef](#)]
29. Huo, R.; Agapiou, A.; Bocos-Bintintan, V.; Brown, L.; Burns, C.; Creaser, C.; Devenport, N.; Gao-Lau, B.; Guallar-Hoyas, C.; Hildebrand, L. The Trapped Human Experiment. *J. Breath Res.* **2011**, *5*, 046006. [[CrossRef](#)] [[PubMed](#)]
30. Lindinger, W.; Hansel, A.; Jordan, A. On-Line Monitoring of Volatile Organic Compounds at Pptv Levels by Means of Proton-Transfer-Reaction Mass Spectrometry (PTR-MS) Medical Applications, Food Control and Environmental Research. *Int. J. Mass Spectrom. Ion Process.* **1998**, *173*, 191–241. [[CrossRef](#)]
31. Righettini, M.; Schmid, A.; Amann, A.; Pratsinis, S.E. Correlations between Blood Glucose and Breath Components from Portable Gas Sensors and PTR-TOF-MS. *J. Breath Res.* **2013**, *7*, 037110. [[CrossRef](#)]
32. Jordan, A.; Hansel, A.; Holzinger, R.; Lindinger, W. Acetonitrile and Benzene in the Breath of Smokers and Non-Smokers Investigated by Proton Transfer Reaction Mass Spectrometry (PTR-MS). *Int. J. Mass Spectrom. Ion Process.* **1995**, *148*, L1–L3. [[CrossRef](#)]
33. Kushch, I.; Schwarz, K.; Schwentner, L.; Baumann, B.; Dzien, A.; Schmid, A.; Unterkofer, K.; Gastl, G.; Španěl, P.; Smith, D. Compounds Enhanced in a Mass Spectrometric Profile of Smokers’ Exhaled Breath versus Non-Smokers as Determined in a Pilot Study Using PTR-MS. *J. Breath Res.* **2008**, *2*, 026002. [[CrossRef](#)]

34. Prazeller, P.; Karl, T.; Jordan, A.; Holzinger, R.; Hansel, A.; Lindinger, W. Quantification of Passive Smoking Using Proton-Transfer-Reaction Mass Spectrometry. *Int. J. Mass Spectrom.* **1998**, *178*, L1–L4. [[CrossRef](#)]
35. Smith, D.; Španěl, P. Direct, Rapid Quantitative Analyses of BVOCs Using SIFT-MS and PTR-MS Obviating Sample Collection. *TrAC Trends Anal. Chem.* **2011**, *30*, 945–959. [[CrossRef](#)]
36. Turner, C.; Španěl, P.; Smith, D. A Longitudinal Study of Ammonia, Acetone and Propanol in the Exhaled Breath of 30 Subjects Using Selected Ion Flow Tube Mass Spectrometry, SIFT-MS. *Physiol. Meas.* **2006**, *27*, 321. [[CrossRef](#)]
37. Turner, C.; Španěl, P.; Smith, D. A Longitudinal Study of Breath Isoprene in Healthy Volunteers Using Selected Ion Flow Tube Mass Spectrometry (SIFT-MS). *Physiol. Meas.* **2005**, *27*, 13. [[CrossRef](#)]
38. Turner, C.; Španěl, P.; Smith, D. A Longitudinal Study of Methanol in the Exhaled Breath of 30 Healthy Volunteers Using Selected Ion Flow Tube Mass Spectrometry, SIFT-MS. *Physiol. Meas.* **2006**, *27*, 637. [[CrossRef](#)]
39. Giannoukos, S.; Brkić, B.; Taylor, S. Analysis of Chlorinated Hydrocarbons in Gas Phase Using a Portable Membrane Inlet Mass Spectrometer. *Anal. Methods* **2016**, *8*, 6607–6615. [[CrossRef](#)]
40. Giannoukos, S.; Joseph, M.J.A.; Taylor, S. Portable Mass Spectrometry for the Direct Analysis and Quantification of Volatile Halogenated Hydrocarbons in the Gas Phase. *Anal. Methods* **2017**, *9*, 910–920. [[CrossRef](#)]
41. Reinecke, T.; Leiminger, M.; Jordan, A.; Wisthaler, A.; Müller, M. Ultrahigh Sensitivity PTR-MS Instrument with a Well-Defined Ion Chemistry. *Anal. Chem.* **2023**, *95*, 11879–11884. [[CrossRef](#)] [[PubMed](#)]
42. Swift, S.J.; Sixtová, N.; Gnioua, M.O.; Španěl, P. A SIFT-MS Study of Positive and Negative Ion Chemistry of the Ortho-, Meta-and Para-Isomers of Cymene, Cresol, and Ethylphenol. *Phys. Chem. Chem. Phys.* **2023**, *25*, 17815–17827. [[CrossRef](#)]
43. Lehnert, A.-S.; Behrendt, T.; Ruecker, A.; Pohnert, G.; Trumbore, S.E. SIFT-MS Optimization for Atmospheric Trace Gas Measurements at Varying Humidity. *Atmospheric Meas. Tech.* **2020**, *13*, 3507–3520. [[CrossRef](#)]
44. Güntner, A.T.; Pineau, N.J.; Mochalski, P.; Wiesenhofer, H.; Agapiou, A.; Mayhew, C.A.; Pratsinis, S.E. Sniffing Entrapped Humans with Sensor Arrays. *Anal. Chem.* **2018**, *90*, 4940–4945. [[CrossRef](#)] [[PubMed](#)]
45. Zang, X.; Pérez, J.J.; Jones, C.M.; Monge, M.E.; McCarty, N.A.; Stecenko, A.A.; Fernández, F.M. Comparison of Ambient and Atmospheric Pressure Ion Sources for Cystic Fibrosis Exhaled Breath Condensate Ion Mobility-Mass Spectrometry Metabolomics. *J. Am. Soc. Mass Spectrom.* **2017**, *28*, 1489–1496. [[CrossRef](#)] [[PubMed](#)]
46. Bregy, L.; Müggler, A.R.; Martinez-Lozano Sinues, P.; García-Gómez, D.; Suter, Y.; Belibasakis, G.N.; Kohler, M.; Schmidlin, P.R.; Zenobi, R. Differentiation of Oral Bacteria in in Vitro Cultures and Human Saliva by Secondary Electrospray Ionization–Mass Spectrometry. *Sci. Rep.* **2015**, *5*, 15163. [[CrossRef](#)]
47. Tejero Rioseras, A.; Singh, K.D.; Nowak, N.; Gaugg, M.T.; Bruderer, T.; Zenobi, R.; Sinues, P.M.-L. Real-Time Monitoring of Tricarboxylic Acid Metabolites in Exhaled Breath. *Anal. Chem.* **2018**, *90*, 6453–6460. [[CrossRef](#)]
48. García-Gómez, D.; Gaisl, T.; Bregy, L.; Sinues, P.M.-L.; Kohler, M.; Zenobi, R. Secondary Electrospray Ionization Coupled to High-Resolution Mass Spectrometry Reveals Tryptophan Pathway Metabolites in Exhaled Human Breath. *Chem. Commun.* **2016**, *52*, 8526–8528. [[CrossRef](#)]
49. Tsiora, A.A.; Plakias, S.; Kokkotis, C.; Veneri, A.; Mina, M.A.; Tsiaikiri, A.; Kitmeridou, S.; Christidi, F.; Gourgoulis, E.; Doskas, T. Artificial Intelligence in the Diagnosis of Neurological Diseases Using Biomechanical and Gait Analysis Data: A Scopus-Based Bibliometric Analysis. *Neurol. Int.* **2025**, *17*, 45. [[CrossRef](#)] [[PubMed](#)]
50. Bastani, H.; Drakopoulos, K.; Gupta, V.; Vlachogiannis, I.; Hadjichristodoulou, C.; Lagiou, P.; Magiorkinis, G.; Paraskevis, D.; Tsiodras, S. Efficient and Targeted COVID-19 Border Testing via Reinforcement Learning. *Nature* **2021**, *599*, 108–113. [[CrossRef](#)]
51. Obermeyer, Z. A Machine-Learning Algorithm to Target COVID Testing of Travellers. *Nature* **2021**, *599*, 34–36. [[CrossRef](#)]
52. Kansizoglou, I.; Kokkotis, C.; Stampoulis, T.; Giannakou, E.; Siaperas, P.; Kallidis, S.; Koutra, M.; Malliou, P.; Michalopoulou, M.; Gasteratos, A. Artificial Intelligence and the Human–Computer Interaction in Occupational Therapy: A Scoping Review. *Algorithms* **2025**, *18*, 276. [[CrossRef](#)]
53. Kokkotis, C.; Kansizoglou, I.; Stampoulis, T.; Giannakou, E.; Siaperas, P.; Kallidis, S.; Koutra, M.; Koutra, C.; Beneka, A.; Bebetsos, E. Artificial Intelligence as Assessment Tool in Occupational Therapy: A Scoping Review. *BioMedInformatics* **2025**, *5*, 22. [[CrossRef](#)]
54. Apostolidis, K.; Kokkotis, C.; Moustakidis, S.; Karakasis, E.; Sakellari, P.; Koutra, C.; Tsitsios, D.; Karatzetzou, S.; Vadikolias, K.; Aggelousis, N. Machine Learning Algorithms for the Prediction of Language and Cognition Rehabilitation Outcomes of Post-Stroke Patients: A Scoping Review. *Hum. Centric Intell. Syst.* **2024**, *4*, 147–160. [[CrossRef](#)]
55. Peters, M.D.; Marnie, C.; Tricco, A.C.; Pollock, D.; Munn, Z.; Alexander, L.; McInerney, P.; Godfrey, C.M.; Khalil, H. Updated Methodological Guidance for the Conduct of Scoping Reviews. *JBI Evid. Synth.* **2021**, *19*, 3–10. [[CrossRef](#)]
56. Tricco, A.C.; Lillie, E.; Zarin, W.; O'Brien, K.K.; Colquhoun, H.; Levac, D.; Moher, D.; Peters, M.D.; Horsley, T.; Weeks, L. PRISMA Extension for Scoping Reviews (PRISMA-ScR): Checklist and Explanation. *Ann. Intern. Med.* **2018**, *169*, 467–473. [[CrossRef](#)]
57. Gudiño-Ochoa, A.; García-Rodríguez, J.A.; Ochoa-Ornelas, R.; Cuevas-Chávez, J.I.; Sánchez-Arias, D.A. Noninvasive Diabetes Detection through Human Breath Using TinyML-Powered E-Nose. *Sensors* **2024**, *24*, 1294. [[CrossRef](#)]
58. Bhaskar, N.; Bairagi, V.; Boonchieng, E.; Munot, M.V. Automated Detection of Diabetes from Exhaled Human Breath Using Deep Hybrid Architecture. *IEEE Access* **2023**, *11*, 51712–51722. [[CrossRef](#)]

59. Li, J.; Hannon, A.; Yu, G.; Idziak, L.A.; Sahasrabhojanee, A.; Govindarajan, P.; Maldonado, Y.A.; Ngo, K.; Abdou, J.P.; Mai, N. Electronic Nose Development and Preliminary Human Breath Testing for Rapid, Non-Invasive COVID-19 Detection. *ACS Sens.* **2023**, *8*, 2309–2318. [[CrossRef](#)]
60. Doguc, O.; Silahtaroglu, G.; Canbolat, Z.N.; Hambarde, K.; Gokay, H.; Ylmaz, M. Diagnosis of Covid-19 via Patient Breath Data Using Artificial Intelligence. *arXiv* **2023**, arXiv:230210180.
61. Snitz, K.; Andelman-Gur, M.; Pinchover, L.; Weissgross, R.; Weissbrod, A.; Mishor, E.; Zoller, R.; Linetsky, V.; Medhanie, A.; Shushan, S. Proof of Concept for Real-Time Detection of SARS CoV-2 Infection with an Electronic Nose. *PLoS ONE* **2021**, *16*, e0252121. [[CrossRef](#)] [[PubMed](#)]
62. Wintjens, A.G.; Hintzen, K.F.; Engelen, S.M.; Lubbers, T.; Savelkoul, P.H.; Wesseling, G.; van der Palen, J.A.; Bouvy, N.D. Applying the Electronic Nose for Pre-Operative SARS-CoV-2 Screening. *Surg. Endosc.* **2021**, *35*, 6671–6678. [[CrossRef](#)] [[PubMed](#)]
63. Binson, V.; Subramoniam, M.; Mathew, L. Detection of COPD and Lung Cancer with Electronic Nose Using Ensemble Learning Methods. *Clin. Chim. Acta* **2021**, *523*, 231–238. [[CrossRef](#)] [[PubMed](#)]
64. Binson, V.; Subramoniam, M.; Mathew, L. Discrimination of COPD and Lung Cancer from Controls through Breath Analysis Using a Self-Developed e-Nose. *J. Breath Res.* **2021**, *15*, 046003. [[CrossRef](#)]
65. Binson, V.; Subramoniam, M.; Mathew, L. Prediction of Lung Cancer with a Sensor Array Based E-Nose System Using Machine Learning Methods. *Microsyst. Technol.* **2024**, *30*, 1421–1434. [[CrossRef](#)]
66. Zhao, L.; Qian, J.; Tian, F.; Liu, R.; Liu, B.; Zhang, S.; Lu, M. A Weighted Discriminative Extreme Learning Machine Design for Lung Cancer Detection by an Electronic Nose System. *IEEE Trans. Instrum. Meas.* **2021**, *70*, 2509709. [[CrossRef](#)]
67. Lee, J.-M.; Choi, E.J.; Chung, J.H.; Lee, K.; Lee, Y.; Kim, Y.-J.; Kim, W.-G.; Yoon, S.H.; Seol, H.Y.; Devaraj, V. A DNA-Derived Phage Nose Using Machine Learning and Artificial Neural Processing for Diagnosing Lung Cancer. *Biosens. Bioelectron.* **2021**, *194*, 113567. [[CrossRef](#)]
68. Kononov, A.; Korotetsky, B.; Jahatspanian, I.; Gubal, A.; Vasiliev, A.; Arsenjev, A.; Nefedov, A.; Barchuk, A.; Gorbunov, I.; Kozyrev, K. Online Breath Analysis Using Metal Oxide Semiconductor Sensors (Electronic Nose) for Diagnosis of Lung Cancer. *J. Breath Res.* **2019**, *14*, 016004. [[CrossRef](#)]
69. Huang, C.-H.; Zeng, C.; Wang, Y.-C.; Peng, H.-Y.; Lin, C.-S.; Chang, C.-J.; Yang, H.-Y. A Study of Diagnostic Accuracy Using a Chemical Sensor Array and a Machine Learning Technique to Detect Lung Cancer. *Sensors* **2018**, *18*, 2845. [[CrossRef](#)] [[PubMed](#)]
70. Rivai, M.; Aulia, D.; Aulia, S. Reducing the Electronic Nose Sensor Array for Asthma Detection Using Firefly Algorithm. *Int. J. Intell. Eng. Syst.* **2024**, *17*, 700–714. [[CrossRef](#)]
71. Abdel-Aziz, M.I.; Brinkman, P.; Vijverberg, S.J.; Neerincx, A.H.; de Vries, R.; Dagelet, Y.W.; Riley, J.H.; Hashimoto, S.; Montuschi, P.; Chung, K.F. eNose Breath Prints as a Surrogate Biomarker for Classifying Patients with Asthma by Atopy. *J. Allergy Clin. Immunol.* **2020**, *146*, 1045–1055. [[CrossRef](#)]
72. Aulia, D.; Sarno, R.; Hidayati, S.C.; Rivai, M. Optimization of the Electronic Nose Sensor Array for Asthma Detection Based on Genetic Algorithm. *IEEE Access* **2023**, *11*, 74924–74935. [[CrossRef](#)]
73. Aulia, D.; Sarno, R.; Hidayati, S.C.; Rosyid, A.N.; Rivai, M. Identification of Chronic Obstructive Pulmonary Disease Using Graph Convolutional Network in Electronic Nose. *Indones. J. Electr. Eng. Comput. Sci.* **2024**, *34*, 264–275. [[CrossRef](#)]
74. Peng, J.; Mei, H.; Yang, R.; Meng, K.; Shi, L.; Zhao, J.; Zhang, B.; Xuan, F.; Wang, T.; Zhang, T. Olfactory Diagnosis Model for Lung Health Evaluation Based on Pyramid Pooling and SHAP-Based Dual Encoders. *ACS Sens.* **2024**, *9*, 4934–4946. [[CrossRef](#)]
75. Tozlu, B.H.; Akmeşe, Ö.F.; Şimşek, C.; Şenel, E. A New Diagnosing Method for Psoriasis from Exhaled Breath. *IEEE Access* **2025**, *13*, 25163–25174. [[CrossRef](#)]
76. Jian, Y.; Zhang, N.; Bi, Y.; Liu, X.; Fan, J.; Wu, W.; Liu, T. TC-Sniffer: A Transformer-CNN Bibranch Framework Leveraging Auxiliary VOCs for Few-Shot UBC Diagnosis via Electronic Noses. *ACS Sens.* **2024**, *10*, 213–224. [[CrossRef](#)] [[PubMed](#)]
77. Gómez, J.K.C.; Vásquez, C.A.C.; Acevedo, C.M.D.; Llecha, J.B. Assessing Data Fusion in Sensory Devices for Enhanced Prostate Cancer Detection Accuracy. *Chemosensors* **2024**, *12*, 228. [[CrossRef](#)]
78. Ghani, M.; Gilanie, G. The IOMT-Based Risk-Free Approach to Lung Disorders Detection from Exhaled Breath Examination. *Intell. Autom. Soft Comput.* **2023**, *36*, 2835–2847. [[CrossRef](#)]
79. Dokter, L.A.; à Nijeholt, J.H.; Rigterink, B.M.; de Lange, N.M.; de Haan, H.H.; van Eijndhoven, H.W.; Joostens, M.; Kruse, A.-J. Development of an Algorithm for Cervical High-Grade Squamous Intraepithelial Lesion Based on Breath Print Analysis. *J. Low. Genit. Tract Dis.* **2023**, *27*, 7–11. [[CrossRef](#)]
80. Ketchanji Mougang, Y.C.; Endale Mangamba, L.-M.; Capuano, R.; Cicacci, F.; Catini, A.; Paolesse, R.; Mbatchou Ngahane, H.B.; Palombi, L.; Di Natale, C. On-Field Test of Tuberculosis Diagnosis through Exhaled Breath Analysis with a Gas Sensor Array. *Biosensors* **2023**, *13*, 570. [[CrossRef](#)]
81. Xuan, W.; Zheng, L.; Bunes, B.R.; Crane, N.; Zhou, F.; Zang, L. Engineering Solutions to Breath Tests Based on an E-Nose System for Silicosis Screening and Early Detection in Miners. *J. Breath Res.* **2022**, *16*, 036001. [[CrossRef](#)]

82. Malikhah, M.; Sarno, R.; Inoue, S.; Ardani, M.S.H.; Purbawa, D.P.; Sabilla, S.I.; Sungkono, K.R.; Faticahah, C.; Cita, D.S.A.B.L.; Prakoeswa, R. A New Approach for Detection of Viral Respiratory Infections Using E-Nose Through Sweat from Armpit with Fully Connected Deep Network. *Int. J. Intell. Eng. Syst.* **2022**, *15*, 394–404. [[CrossRef](#)]
83. Binson, V.; Subramoniam, M.; Sunny, Y.; Mathew, L. Prediction of Pulmonary Diseases with Electronic Nose Using SVM and XGBoost. *IEEE Sens. J.* **2021**, *21*, 20886–20895. [[CrossRef](#)]
84. Mahdavi, H.; Rahbarpour, S.; Hosseini-Golgoo, S.M.; Jamaati, H. A Single Gas Sensor Assisted by Machine Learning Algorithms for Breath-Based Detection of COPD: A Pilot Study. *Sens. Actuators Phys.* **2024**, *376*, 115650. [[CrossRef](#)]
85. Karthick, G.; Pankajavalli, P. Chronic Obstructive Pulmonary Disease Prediction Using Internet of Things-Spiro System and Fuzzy-Based Quantum Neural Network Classifier. *Theor. Comput. Sci.* **2023**, *941*, 55–76. [[CrossRef](#)]
86. Avian, C.; Mahali, M.I.; Putro, N.A.S.; Prakosa, S.W.; Leu, J.-S. Fx-Net and PureNet: Convolutional Neural Network Architecture for Discrimination of Chronic Obstructive Pulmonary Disease from Smokers and Healthy Subjects through Electronic Nose Signals. *Comput. Biol. Med.* **2022**, *148*, 105913. [[CrossRef](#)]
87. El-Magd, L.M.A.; Dahy, G.; Farrag, T.A.; Darwish, A.; Hassnien, A.E. An Interpretable Deep Learning Based Approach for Chronic Obstructive Pulmonary Disease Using Explainable Artificial Intelligence. *Int. J. Inf. Technol.* **2024**, *17*, 4077–4092. [[CrossRef](#)]
88. Suresh, K.; Prabha, R.; Hemavathy, N.; Sivarajeswari, S.; Gokulakrishnan, D. A Machine Learning Approach for Human Breath Diagnosis with Soft Sensors. *Comput. Electr. Eng.* **2022**, *100*, 107945. [[CrossRef](#)]
89. Połaka, I.; Mežmale, L.; Anarkulova, L.; Kononova, E.; Vilkoite, I.; Veliks, V.; Leščinska, A.M.; Stonāns, I.; Pēcklins, A.; Tolmanis, I. The Detection of Colorectal Cancer through Machine Learning-Based Breath Sensor Analysis. *Diagnostics* **2023**, *13*, 3355. [[CrossRef](#)] [[PubMed](#)]
90. Polaka, I.; Bhandari, M.P.; Mezmale, L.; Anarkulova, L.; Veliks, V.; Sivins, A.; Lescinska, A.M.; Tolmanis, I.; Vilkoite, I.; Ivanovs, I. Modular Point-of-Care Breath Analyzer and Shape Taxonomy-Based Machine Learning for Gastric Cancer Detection. *Diagnostics* **2022**, *12*, 491. [[CrossRef](#)]
91. Pérez-Sánchez, C.; Barroja, N.; Pantaleão, L.C.; López-Sánchez, L.M.; Ozanne, S.E.; Jurado-Gámez, B.; Aranda, E.; Lopez-Pedrera, C.; Rodríguez-Ariza, A. Clinical Utility of microRNAs in Exhaled Breath Condensate as Biomarkers for Lung Cancer. *J. Pers. Med.* **2021**, *11*, 111. [[CrossRef](#)]
92. Lee, B.; Lee, J.; Lee, J.-O.; Hwang, Y.; Bahn, H.-K.; Park, I.; Jheon, S.; Lee, D.-S. Breath Analysis System with Convolutional Neural Network (CNN) for Early Detection of Lung Cancer. *Sens. Actuators B Chem.* **2024**, *409*, 135578. [[CrossRef](#)]
93. Lekshmy, S.; Sridhar, K.; Roberts, M.K. Analyzing the Performance of a Bio-Sensor Integrated Improved Blended Learning Model for Accurate Pneumonia Prediction. *Results Eng.* **2024**, *22*, 102063. [[CrossRef](#)]
94. Nurputra, D.K.; Kusumaatmaja, A.; Hakim, M.S.; Hidayat, S.N.; Julian, T.; Sumanto, B.; Mahendradhata, Y.; Saktiawati, A.M.I.; Wasisto, H.S.; Triyana, K. Fast and Noninvasive Electronic Nose for Sniffing out COVID-19 Based on Exhaled Breath-Print Recognition. *NPJ Digit. Med.* **2022**, *5*, 115. [[CrossRef](#)]
95. Hidayat, S.N.; Julian, T.; Dharmawan, A.B.; Puspita, M.; Chandra, L.; Rohman, A.; Julia, M.; Rianjanu, A.; Nurputra, D.K.; Triyana, K. Hybrid Learning Method Based on Feature Clustering and Scoring for Enhanced COVID-19 Breath Analysis by an Electronic Nose. *Artif. Intell. Med.* **2022**, *129*, 102323. [[CrossRef](#)]
96. Shan, B.; Broza, Y.Y.; Li, W.; Wang, Y.; Wu, S.; Liu, Z.; Wang, J.; Gui, S.; Wang, L.; Zhang, Z. Multiplexed Nanomaterial-Based Sensor Array for Detection of COVID-19 in Exhaled Breath. *ACS Nano* **2020**, *14*, 12125–12132. [[CrossRef](#)] [[PubMed](#)]
97. van der Sar, I.G.; van Jaarsveld, N.; Spiekerman, I.A.; Toxopeus, F.J.; Langens, Q.L.; Wijsenbeek, M.S.; Dauwels, J.; Moor, C.C. Evaluation of Different Classification Methods Using Electronic Nose Data to Diagnose Sarcoidosis. *J. Breath Res.* **2023**, *17*, 047104. [[CrossRef](#)]
98. Bhaskar, N.; Borhade, R.R.; Barekar, S.; Bachute, M.; Bairagi, V. CNN-CatBoost Ensemble Deep Learning Model for Enhanced Disease Detection and Classification of Kidney Disease. *Indones. J. Electr. Eng. Comput. Sci.* **2024**, *34*, 144–151. [[CrossRef](#)]
99. Bhaskar, N.; Ajithkumar, A.M.; Tupe-Waghmare, P. An Efficient Convolutional Neural Network-Extreme Gradient Boosting Hybrid Deep Learning Model for Disease Detection Applications. *Int. J. Electr. Comput. Eng. IJECE* **2024**, *14*, 2035–2042. [[CrossRef](#)]
100. Lekha, S.; Suchetha, M. Real-Time Non-Invasive Detection and Classification of Diabetes Using Modified Convolution Neural Network. *IEEE J. Biomed. Health Inform.* **2017**, *22*, 1630–1636. [[CrossRef](#)]
101. Baedorf-Kassis, E.N.; Glowala, J.; Póka, K.B.; Wadehn, F.; Meyer, J.; Talmor, D. Reverse Triggering Neural Network and Rules-Based Automated Detection in Acute Respiratory Distress Syndrome. *J. Crit. Care* **2023**, *75*, 154256. [[CrossRef](#)]
102. Wijbenga, N.; Hoek, R.A.; Mathot, B.J.; Seghers, L.; Moor, C.C.; Aerts, J.G.; Bos, D.; Manintveld, O.C.; Hellemons, M.E. Diagnostic Performance of Electronic Nose Technology in Chronic Lung Allograft Dysfunction. *J. Heart Lung Transplant.* **2023**, *42*, 236–245. [[CrossRef](#)]
103. Fan, L.; Chen, Y.; Chen, Y.; Wang, L.; Liang, S.; Cheng, K.; Pei, Y.; Feng, Y.; Li, Q.; He, M. Discovery and Analysis of the Relationship between Organic Components in Exhaled Breath and Bronchiectasis. *J. Breath Res.* **2024**, *19*, 016003. [[CrossRef](#)]
104. Roquencourt, C.; Salvator, H.; Bardin, E.; Lamy, E.; Farfour, E.; Naline, E.; Devillier, P.; Grassin-Delyle, S. Enhanced Real-Time Mass Spectrometry Breath Analysis for the Diagnosis of COVID-19. *ERJ Open Res.* **2023**, *9*, 00206–2023. [[CrossRef](#)]

105. Liangou, A.; Tasoglou, A.; Huber, H.J.; Wistrom, C.; Brody, K.; Menon, P.G.; Bebekoski, T.; Menschel, K.; Davidson-Fiedler, M.; DeMarco, K. A Method for the Identification of COVID-19 Biomarkers in Human Breath Using Proton Transfer Reaction Time-of-Flight Mass Spectrometry. *EClinicalMedicine* **2021**, *42*, 101207. [CrossRef] [PubMed]
106. Grassin-Delyle, S.; Roquencourt, C.; Moine, P.; Saffroy, G.; Carn, S.; Heming, N.; Fleuriet, J.; Salvator, H.; Naline, E.; Couderc, L.-J. Metabolomics of Exhaled Breath in Critically Ill COVID-19 Patients: A Pilot Study. *EBioMedicine* **2021**, *63*, 103154. [CrossRef] [PubMed]
107. Weber, R.; Streckenbach, B.; Welti, L.; Inci, D.; Kohler, M.; Perkins, N.; Zenobi, R.; Micic, S.; Moeller, A. Online Breath Analysis with SESI/HRMS for Metabolic Signatures in Children with Allergic Asthma. *Front. Mol. Biosci.* **2023**, *10*, 1154536. [CrossRef]
108. Fu, L.; Wang, L.; Wang, H.; Yang, M.; Yang, Q.; Lin, Y.; Guan, S.; Deng, Y.; Liu, L.; Li, Q. A Cross-Sectional Study: A Breathomics Based Pulmonary Tuberculosis Detection Method. *BMC Infect. Dis.* **2023**, *23*, 148. [CrossRef] [PubMed]
109. Rai, S.N.; Das, S.; Pan, J.; Mishra, D.C.; Fu, X.-A. Multigroup Prediction in Lung Cancer Patients and Comparative Controls Using Signature of Volatile Organic Compounds in Breath Samples. *PLoS ONE* **2022**, *17*, e0277431. [CrossRef]
110. Tsou, P.-H.; Lin, Z.-L.; Pan, Y.-C.; Yang, H.-C.; Chang, C.-J.; Liang, S.-K.; Wen, Y.-F.; Chang, C.-H.; Chang, L.-Y.; Yu, K.-L. Exploring Volatile Organic Compounds in Breath for High-Accuracy Prediction of Lung Cancer. *Cancers* **2021**, *13*, 1431. [CrossRef] [PubMed]
111. Butcher, J.B.; Rutter, A.V.; Wootton, A.J.; Day, C.R.; Sulé-Suso, J. *Artificial Neural Network Analysis of Volatile Organic Compounds for the Detection of Lung Cancer*; Springer: Berlin/Heidelberg, Germany, 2017; pp. 183–190.
112. Chen, D.; Bryden, W.A.; Wood, R. Detection of Tuberculosis by the Analysis of Exhaled Breath Particles with High-Resolution Mass Spectrometry. *Sci. Rep.* **2020**, *10*, 7647. [CrossRef]
113. Zhang, J.; He, X.; Guo, X.; Wang, J.; Gong, X.; Jiao, D.; Chen, H.; Liu, Z. Identification Potential Biomarkers for Diagnosis, and Progress of Breast Cancer by Using High-Pressure Photon Ionization Time-of-Flight Mass Spectrometry. *Anal. Chim. Acta* **2024**, *1320*, 342883. [CrossRef]
114. Mustafina, M.; Silantyev, A.; Krasovskiy, S.; Chernyak, A.; Naumenko, Z.; Suvorov, A.; Gognieva, D.; Abdullaev, M.; Bektimirova, A.; Bykova, A. Exhaled Breath Analysis in Adult Patients with Cystic Fibrosis by Real-Time Proton Mass Spectrometry. *Clin. Chim. Acta* **2024**, *560*, 119733. [CrossRef]
115. Jiao, B.; Zhang, S.; Bei, Y.; Bu, G.; Yuan, L.; Zhu, Y.; Yang, Q.; Xu, T.; Zhou, L.; Liu, Q. A Detection Model for Cognitive Dysfunction Based on Volatile Organic Compounds from a Large Chinese Community Cohort. *Alzheimers Dement.* **2023**, *19*, 4852–4862. [CrossRef]
116. Miller-Atkins, G.; Acevedo-Moreno, L.; Grove, D.; Dweik, R.A.; Tonelli, A.R.; Brown, J.M.; Allende, D.S.; Aucejo, F.; Rotroff, D.M. Breath Metabolomics Provides an Accurate and Noninvasive Approach for Screening Cirrhosis, Primary, and Secondary Liver Tumors. *Hepatol. Commun.* **2020**, *4*, 1041–1055. [CrossRef]
117. Henning, D.; Lüno, M.; Jiang, C.; Meyer-Lotz, G.; Hoeschen, C.; Frodl, T. Gut–Brain Axis Volatile Organic Compounds Derived from Breath Distinguish between Schizophrenia and Major Depressive Disorder. *J. Psychiatry Neurosci.* **2023**, *48*, E117–E125. [CrossRef]
118. Taylor, M.J.; Chitwood, C.P.; Xie, Z.; Miller, H.A.; van Berkel, V.H.; Fu, X.-A.; Frieboes, H.B.; Suliman, S.A. Disease Diagnosis and Severity Classification in Pulmonary Fibrosis Using Carbonyl Volatile Organic Compounds in Exhaled Breath. *Respir. Med.* **2024**, *222*, 107534. [CrossRef]
119. Xiang, C.; Yang, H.; Zhao, Z.; Deng, F.; Lv, Y.; Yang, Y.; Duan, Y.; Li, W.; Hu, B. Volatolomics Analysis of Exhaled Breath and Gastric-Endoluminal Gas for Distinguishing Early Upper Gastrointestinal Cancer from Benign. *J. Breath Res.* **2023**, *17*, 036004. [CrossRef] [PubMed]
120. Hirdman, G.; Bodén, E.; Kjellström, S.; Fraenkel, C.-J.; Olm, F.; Hallgren, O.; Lindstedt, S. Proteomic Characteristics and Diagnostic Potential of Exhaled Breath Particles in Patients with COVID-19. *Clin. Proteom.* **2023**, *20*, 13. [CrossRef] [PubMed]
121. Xue, C.; Xu, X.; Liu, Z.; Zhang, Y.; Xu, Y.; Niu, J.; Jin, H.; Xiong, W.; Cui, D. Intelligent COVID-19 Screening Platform Based on Breath Analysis. *J. Breath Res.* **2022**, *17*, 016005. [CrossRef]
122. Woollam, M.; Angarita-Rivera, P.; Siegel, A.P.; Kalra, V.; Kapoor, R.; Agarwal, M. Exhaled VOCs Can Discriminate Subjects with COVID-19 from Healthy Controls. *J. Breath Res.* **2022**, *16*, 036002. [CrossRef]
123. Zhang, P.; Ren, T.; Chen, H.; Li, Q.; He, M.; Feng, Y.; Wang, L.; Huang, T.; Yuan, J.; Deng, G. A Feasibility Study of Covid-19 Detection Using Breath Analysis by High-Pressure Photon Ionization Time-of-Flight Mass Spectrometry. *J. Breath Res.* **2022**, *16*, 046009. [CrossRef] [PubMed]
124. Nazir, N.U.; Abbas, S.R. Identification of Phenol 2, 2-Methylene Bis, 6 [1, 1-D] as Breath Biomarker of Hepatocellular Carcinoma (HCC) Patients and Its Electrochemical Sensing: E-Nose Biosensor for HCC. *Anal. Chim. Acta* **2023**, *1242*, 340752. [CrossRef]
125. Gashimova, E.; Temerdashev, A.; Porkhanov, V.; Polyakov, I.; Perunov, D.; Dmitrieva, E. Non-Invasive Exhaled Breath and Skin Analysis to Diagnose Lung Cancer: Study of Age Effect on Diagnostic Accuracy. *ACS Omega* **2022**, *7*, 42613–42628. [CrossRef] [PubMed]
126. Koureas, M.; Kalompatsios, D.; Amoutzias, G.D.; Hadjichristodoulou, C.; Gourgoulianis, K.; Tsakalof, A. Comparison of Targeted and Untargeted Approaches in Breath Analysis for the Discrimination of Lung Cancer from Benign Pulmonary Diseases and Healthy Persons. *Molecules* **2021**, *26*, 2609. [CrossRef] [PubMed]

127. Koureas, M.; Kirgou, P.; Amoutzias, G.; Hadjichristodoulou, C.; Gourgoulianis, K.; Tsakalof, A. Target Analysis of Volatile Organic Compounds in Exhaled Breath for Lung Cancer Discrimination from Other Pulmonary Diseases and Healthy Persons. *Metabolites* **2020**, *10*, 317. [CrossRef] [PubMed]
128. Pelit, F.; Goksel, O.; Dizzdas, T.N.; Arin, A.; Ozgur, S.; Erbas, I.; Gursoy, A.; Ordin, B.; Karakus, H.S.; Ertas, F.N. Identification of Volatile Biomarkers in Exhaled Breath by Polythiophene Solid Phase Microextraction Fiber for Disease Diagnosis Using GC–MS. *Microchem. J.* **2024**, *207*, 112067. [CrossRef]
129. Cheng, H.R.; van Vorstenbosch, R.W.; Pachen, D.M.; Meulen, L.W.; Straathof, J.W.A.; Dallinga, J.W.; Jonkers, D.M.; Mascllee, A.A.; van Schooten, F.-J.; Mujagic, Z. Detecting Colorectal Adenomas and Cancer Using Volatile Organic Compounds in Exhaled Breath: A Proof-of-Principle Study to Improve Screening. *Clin. Transl. Gastroenterol.* **2022**, *13*, e00518. [CrossRef]
130. Patnaik, R.K.; Lin, Y.-C.; Ho, M.C.; Yeh, J.A. Selection of Consistent Breath Biomarkers of Abnormal Liver Function Using Feature Selection: A Pilot Study. *Health Technol.* **2023**, *13*, 957–969. [CrossRef]
131. Patnaik, R.K.; Lin, Y.-C.; Agarwal, A.; Ho, M.-C.; Yeh, J.A. A Pilot Study for the Prediction of Liver Function Related Scores Using Breath Biomarkers and Machine Learning. *Sci. Rep.* **2022**, *12*, 2032. [CrossRef]
132. Khan, M.S.; Cuda, S.; Karere, G.M.; Cox, L.A.; Bishop, A.C. Breath Biomarkers of Insulin Resistance in Pre-Diabetic Hispanic Adolescents with Obesity. *Sci. Rep.* **2022**, *12*, 339. [CrossRef]
133. Di Gilio, A.; Catino, A.; Lombardi, A.; Palmisani, J.; Facchini, L.; Mongelli, T.; Varesano, N.; Bellotti, R.; Galetta, D.; de Gennaro, G. Breath Analysis for Early Detection of Malignant Pleural Mesothelioma: Volatile Organic Compounds (VOCs) Determination and Possible Biochemical Pathways. *Cancers* **2020**, *12*, 1262. [CrossRef]
134. Beccaria, M.; Bobak, C.; Maitshotlo, B.; Mellors, T.R.; Purcaro, G.; Franchina, F.A.; Rees, C.A.; Nasir, M.; Black, A.; Hill, J.E. Exhaled Human Breath Analysis in Active Pulmonary Tuberculosis Diagnostics by Comprehensive Gas Chromatography-Mass Spectrometry and Chemometric Techniques. *J. Breath Res.* **2018**, *13*, 016005. [CrossRef] [PubMed]
135. Bobak, C.A.; Kang, L.; Workman, L.; Bateman, L.; Khan, M.S.; Prins, M.; May, L.; Franchina, F.A.; Baard, C.; Nicol, M.P. Breath Can Discriminate Tuberculosis from Other Lower Respiratory Illness in Children. *Sci. Rep.* **2021**, *11*, 2704. [CrossRef]
136. Sharma, R.; Zang, W.; Zhou, M.; Schafer, N.; Begley, L.A.; Huang, Y.J.; Fan, X. Real Time Breath Analysis Using Portable Gas Chromatography for Adult Asthma Phenotypes. *Metabolites* **2021**, *11*, 265. [CrossRef]
137. Wieczorek, M.; Weston, A.; Ledenko, M.; Thomas, J.N.; Carter, R.; Patel, T. A Deep Learning Approach for Detecting Liver Cirrhosis from Volatolomic Analysis of Exhaled Breath. *Front. Med.* **2022**, *9*, 992703. [CrossRef]
138. Thomas, J.N.; Roopkumar, J.; Patel, T. Machine Learning Analysis of Volatolomic Profiles in Breath Can Identify Non-Invasive Biomarkers of Liver Disease: A Pilot Study. *PLoS ONE* **2021**, *16*, e0260098. [CrossRef] [PubMed]
139. Chen, H.; Qi, X.; Zhang, L.; Li, X.; Ma, J.; Zhang, C.; Feng, H.; Yao, M. COVID-19 Screening Using Breath-Borne Volatile Organic Compounds. *J. Breath Res.* **2021**, *15*, 047104. [CrossRef]
140. Mentel, S.; Gallo, K.; Wagendorf, O.; Preissner, R.; Nahles, S.; Heiland, M.; Preissner, S. Prediction of Oral Squamous Cell Carcinoma Based on Machine Learning of Breath Samples: A Prospective Controlled Study. *BMC Oral Health* **2021**, *21*, 500. [CrossRef]
141. Sukaram, T.; Apiparakoon, T.; Tiyyarattanachai, T.; Ariyaskul, D.; Kulkraisri, K.; Marukatat, S.; Rerknimitr, R.; Chaiteerakij, R. VOCs from Exhaled Breath for the Diagnosis of Hepatocellular Carcinoma. *Diagnostics* **2023**, *13*, 257. [CrossRef]
142. Golyak, I.S.; Anfimov, D.R.; Demkin, P.P.; Berezhanskiy, P.V.; Nebritova, O.A.; Morozov, A.N.; Fufurin, I.L. A Hybrid Learning Approach to Better Classify Exhaled Breath's Infrared Spectra: A Noninvasive Optical Diagnosis for Socially Significant Diseases. *J. Biophotonics* **2024**, *17*, e202400151. [CrossRef] [PubMed]
143. Liang, Q.; Chan, Y.-C.; Toscano, J.; Bjorkman, K.K.; Leinwand, L.A.; Parker, R.; Nozik, E.S.; Nesbitt, D.J.; Ye, J. Breath Analysis by Ultra-Sensitive Broadband Laser Spectroscopy Detects SARS-CoV-2 Infection. *J. Breath Res.* **2023**, *17*, 036001. [CrossRef]
144. Shlomo, I.B.; Frankenthal, H.; Laor, A.; Greenhut, A.K. Detection of SARS-CoV-2 Infection by Exhaled Breath Spectral Analysis: Introducing a Ready-to-Use Point-of-Care Mass Screening Method. *EClinicalMedicine* **2022**, *45*, 101308. [CrossRef]
145. Cusack, R.P.; Larracy, R.; Morrell, C.B.; Ranjbar, M.; Le Roux, J.; Whetstone, C.E.; Boudreau, M.; Poitras, P.F.; Srinathan, T.; Cheng, E. Machine Learning Enabled Detection of COVID-19 Pneumonia Using Exhaled Breath Analysis: A Proof-of-Concept Study. *J. Breath Res.* **2024**, *18*, 026009. [CrossRef]
146. Borisov, A.V.; Syrkina, A.G.; Kuzmin, D.A.; Ryabov, V.V.; Boyko, A.A.; Zaharova, O.; Zasedatel, V.S.; Kistenev, Y.V. Application of Machine Learning and Laser Optical-Acoustic Spectroscopy to Study the Profile of Exhaled Air Volatile Markers of Acute Myocardial Infarction. *J. Breath Res.* **2021**, *15*, 027104. [CrossRef]
147. Kistenev, Y.V.; Borisov, A.V.; Nikolaev, V.V.; Vrazhnov, D.A.; Kuzmin, D.A. Laser Photoacoustic Spectroscopy Applications in Breathomics. *J. Biomed. Photonics Eng.* **2019**, *5*, 010303. [CrossRef]
148. Xie, X.; Yu, W.; Wang, L.; Yang, J.; Tu, X.; Liu, X.; Liu, S.; Zhou, H.; Chi, R.; Huang, Y. SERS-Based AI Diagnosis of Lung and Gastric Cancer via Exhaled Breath. *Spectrochim. Acta Part A Mol. Biomol. Spectrosc.* **2024**, *314*, 124181. [CrossRef]
149. Xu, J.; Xu, Y.; Li, J.; Zhao, J.; Jian, X.; Xu, J.; Gao, Z.; Song, Y.-Y. Construction of High-Active SERS Cavities in a TiO₂ Nanochannels-Based Membrane: A Selective Device for Identifying Volatile Aldehyde Biomarkers. *ACS Sens.* **2023**, *8*, 3487–3497. [CrossRef] [PubMed]

150. Aslam, M.A.; Xue, C.; Chen, Y.; Zhang, A.; Liu, M.; Wang, K.; Cui, D. Breath Analysis Based Early Gastric Cancer Classification from Deep Stacked Sparse Autoencoder Neural Network. *Sci. Rep.* **2021**, *11*, 4014. [[CrossRef](#)]
151. Nguyen, T.M.; Chung, J.H.; Bak, G.-H.; Kim, Y.H.; Kim, M.; Kim, Y.-J.; Kwon, R.J.; Choi, E.-J.; Kim, K.H.; Kim, Y.S. Multiarray Biosensor for Diagnosing Lung Cancer Based on Gap Plasmonic Color Films. *ACS Sens.* **2022**, *8*, 167–175. [[CrossRef](#)] [[PubMed](#)]
152. Picciariello, A.; Dezi, A.; Vincenzi, L.; Spampinato, M.G.; Zang, W.; Riahi, P.; Scott, J.; Sharma, R.; Fan, X.; Altomare, D.F. Colorectal Cancer Diagnosis through Breath Test Using a Portable Breath Analyzer—Preliminary Data. *Sensors* **2024**, *24*, 2343. [[CrossRef](#)]
153. Zhou, M.; Sharma, R.; Zhu, H.; Li, Z.; Li, J.; Wang, S.; Bisco, E.; Massey, J.; Pennington, A.; Sjoding, M. Rapid Breath Analysis for Acute Respiratory Distress Syndrome Diagnostics Using a Portable Two-Dimensional Gas Chromatography Device. *Anal. Bioanal. Chem.* **2019**, *411*, 6435–6447. [[CrossRef](#)]

Disclaimer/Publisher's Note: The statements, opinions and data contained in all publications are solely those of the individual author(s) and contributor(s) and not of MDPI and/or the editor(s). MDPI and/or the editor(s) disclaim responsibility for any injury to people or property resulting from any ideas, methods, instructions or products referred to in the content.